Colloidal nanoparticles as advanced biological sensors,
Philip D. Howes, Rona Chandrawati, Molly M. Stevens*
P. D. Howes *et al*., *Science* **346**, 53 (2014)

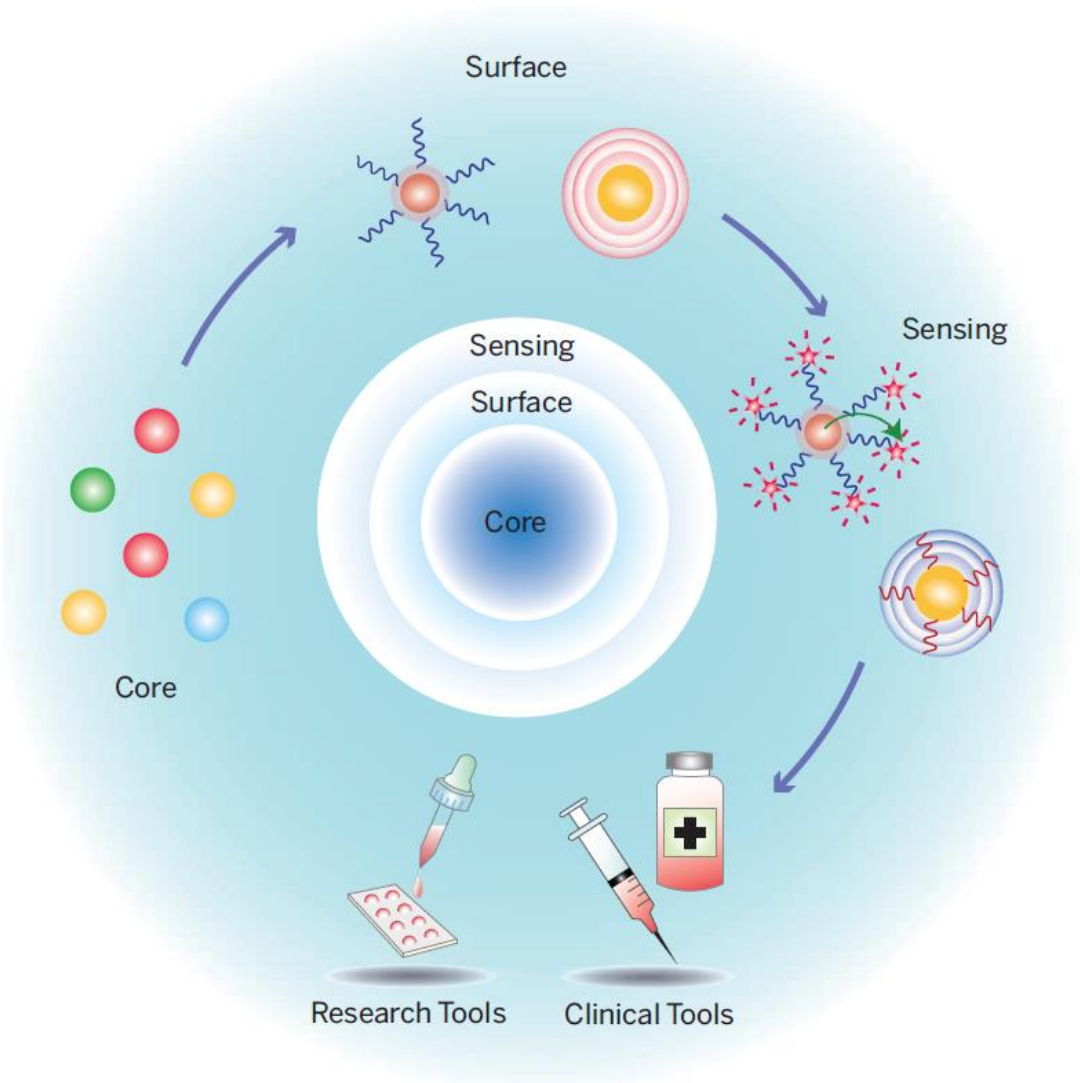

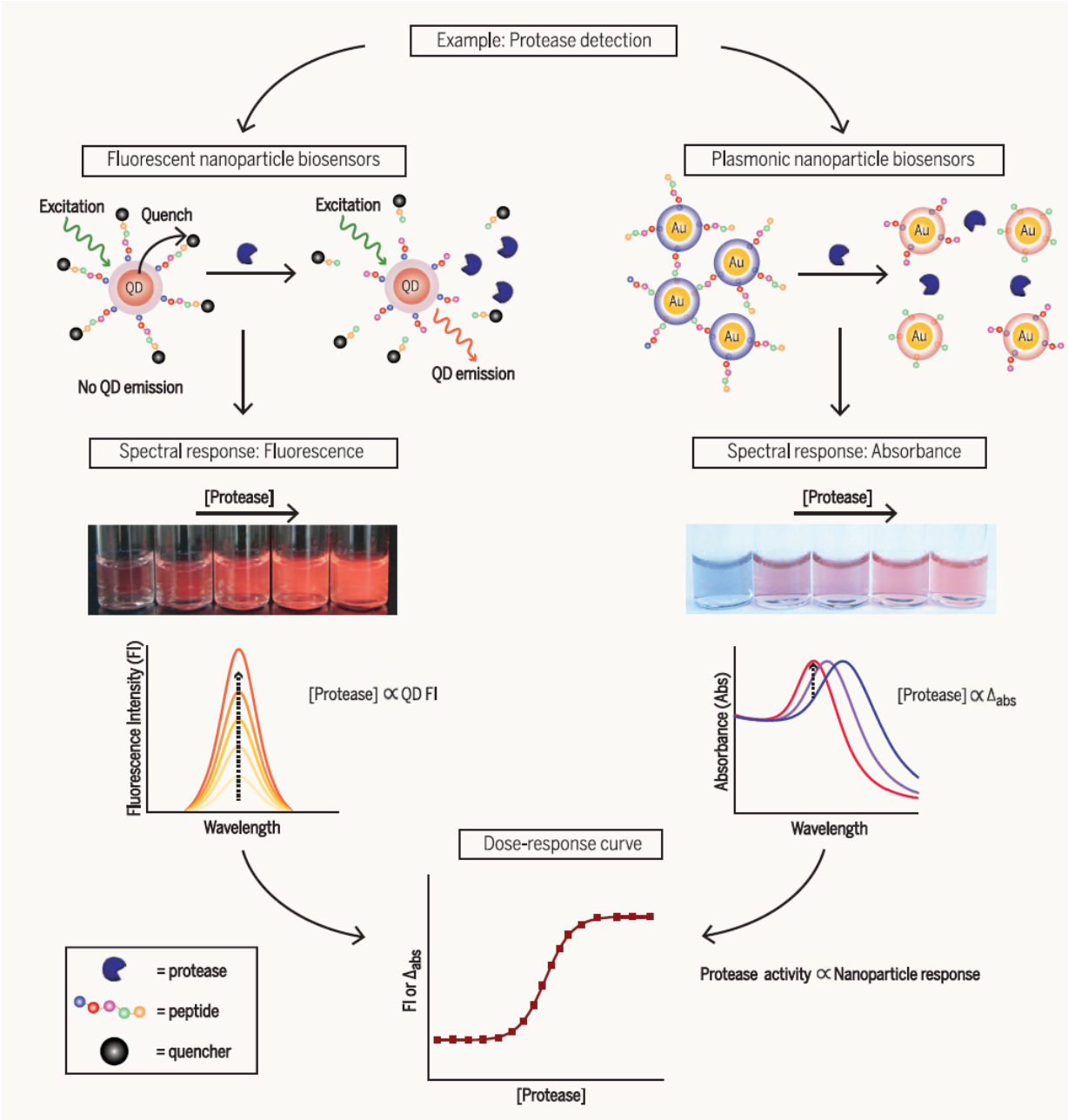

P. D. Howes *et al.*, *Science* **346**, 53 (2014)

Quantum dot bioconjugates for imaging, labelling and sensing

H. Mattoussi, *Nature Mater*. **2005,** *4*, 435.

- Applications in cellular labelling, deep-tissue imaging, assay labelling and as efficient fluorescence resonance energy transfer donors.
- High quantum yield, high molar extinction coefficients (~10–100× that of organic dyes)
- Broad absorption with narrow, symmetric photoluminescence (PL) spectra (full-width at half-maximum ~25–40 nm) spanning the UV to near-infrared, large effective Stokes shifts
- High resistance to photobleaching
- Exceptional resistance to photo- and chemical degradation
- Size-tune fluorescent emission as a function of core size
- Broad excitation spectra, which allow excitation of mixed QD populations at a single wavelength far removed (>100 nm) from their respective emissions → 'multiplexing' (simultaneous detection of multiple signals).

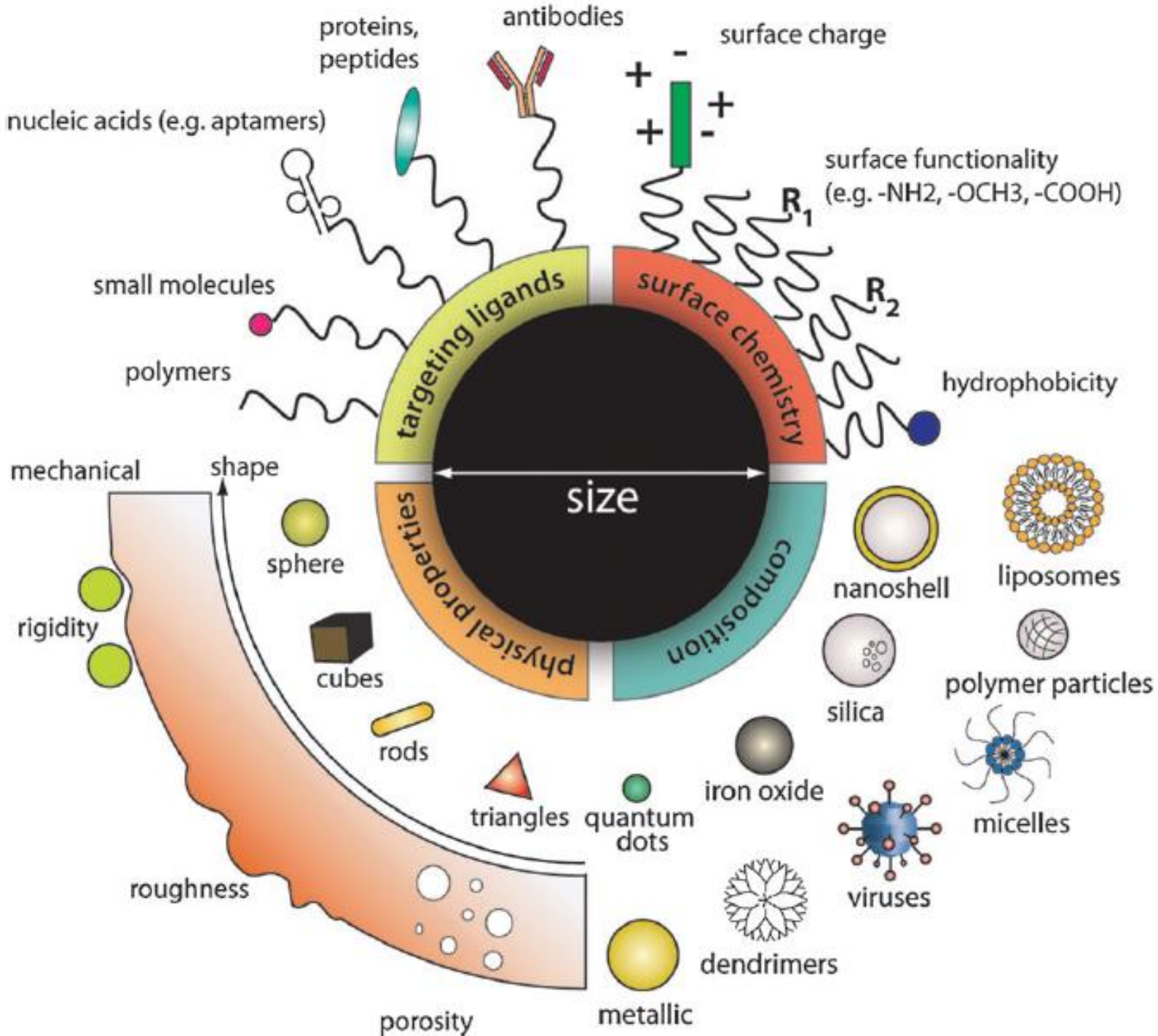
proteins, peptides
antibodies
surface charge
nucleic acids (e.g. aptamers)
surface functionality (e.g. -NH2, -OCH3, -COOH)
R1
R2
small molecules
polymers
targeting ligands
surface chemistry
hydrophobicity
mechanical
shape
size
sphere
physical properties
composition
nanoshell
liposomes
rigidity
cubes
silica
polymer particles
rods
iron oxide
triangles
quantum dots
micelles
viruses
roughness
dendrimers
metallic
porosity

Comparison of rhodamine red/DsRed2 spectral properties to those of QDs highlighting how multiple narrow, symmetric QD emissions can be used in the same spectral window as that of an organic dye.

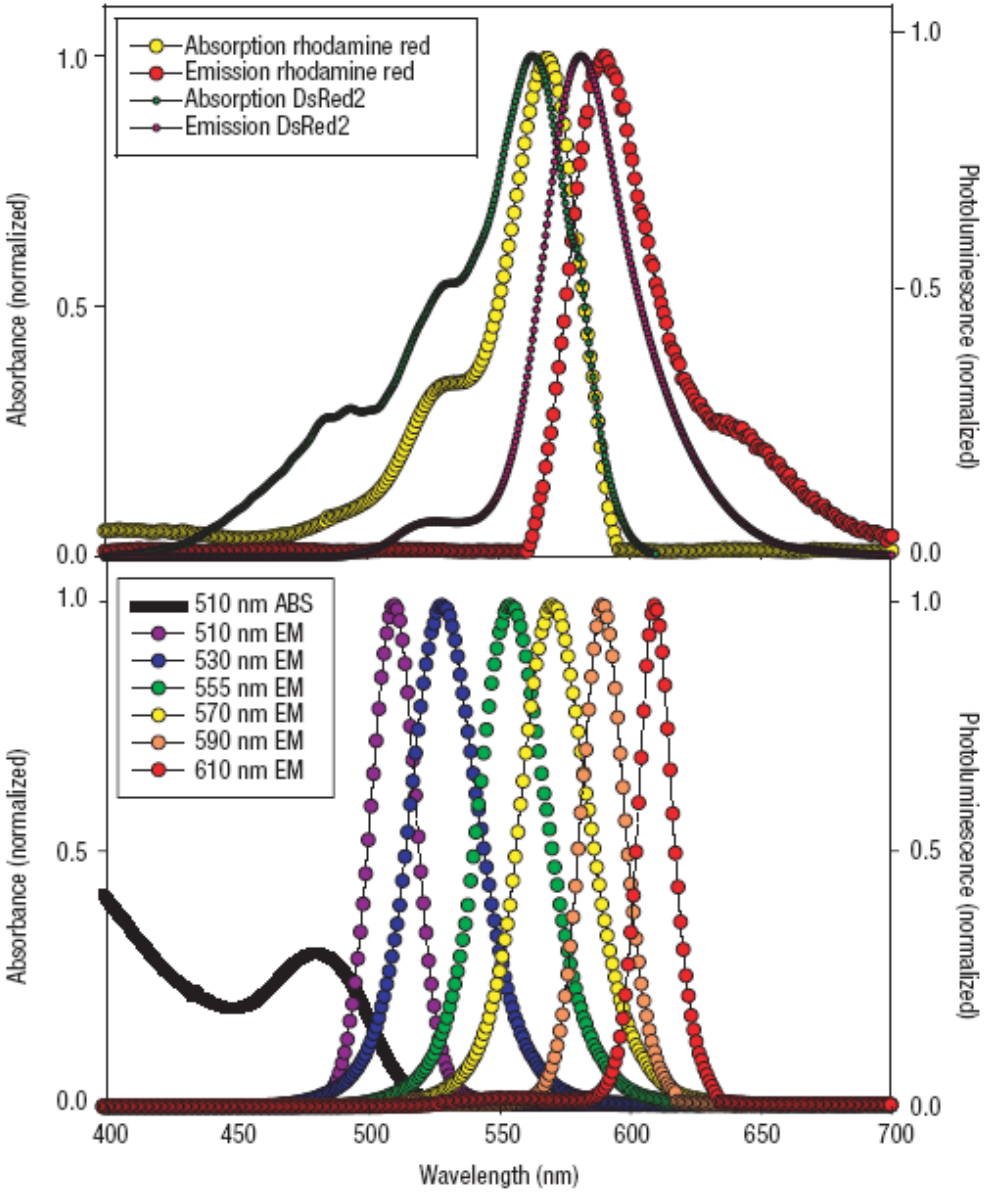

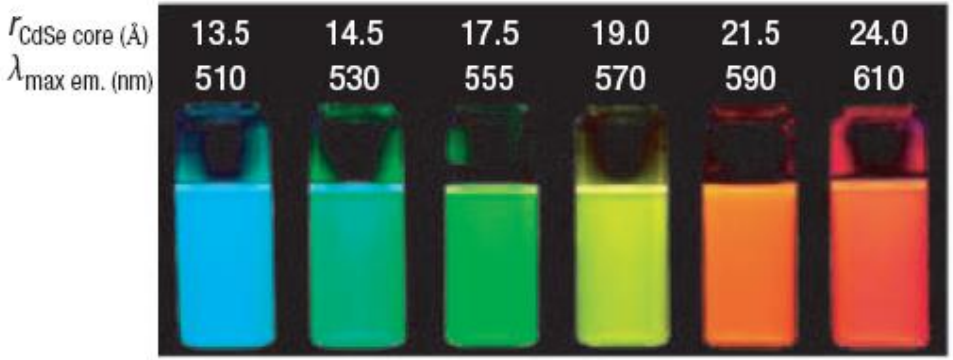

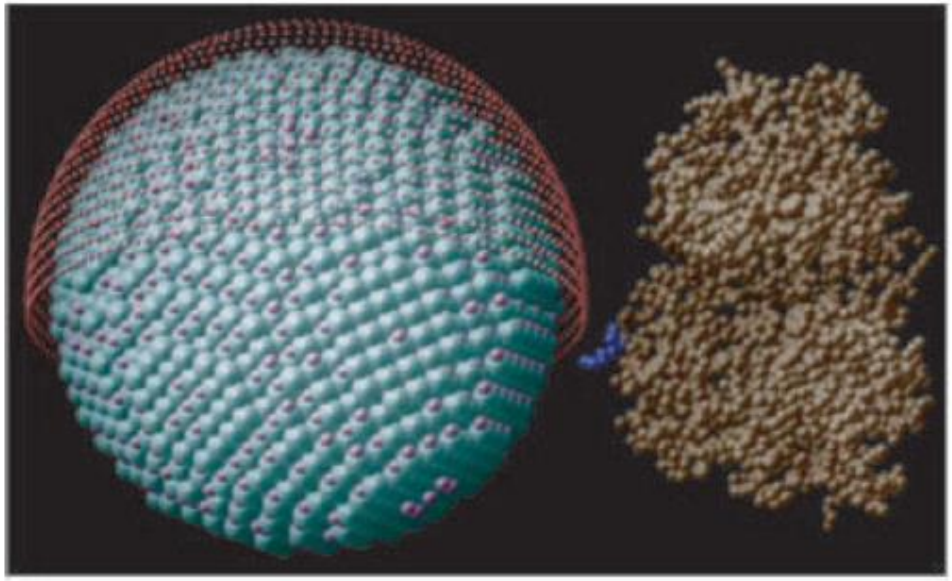

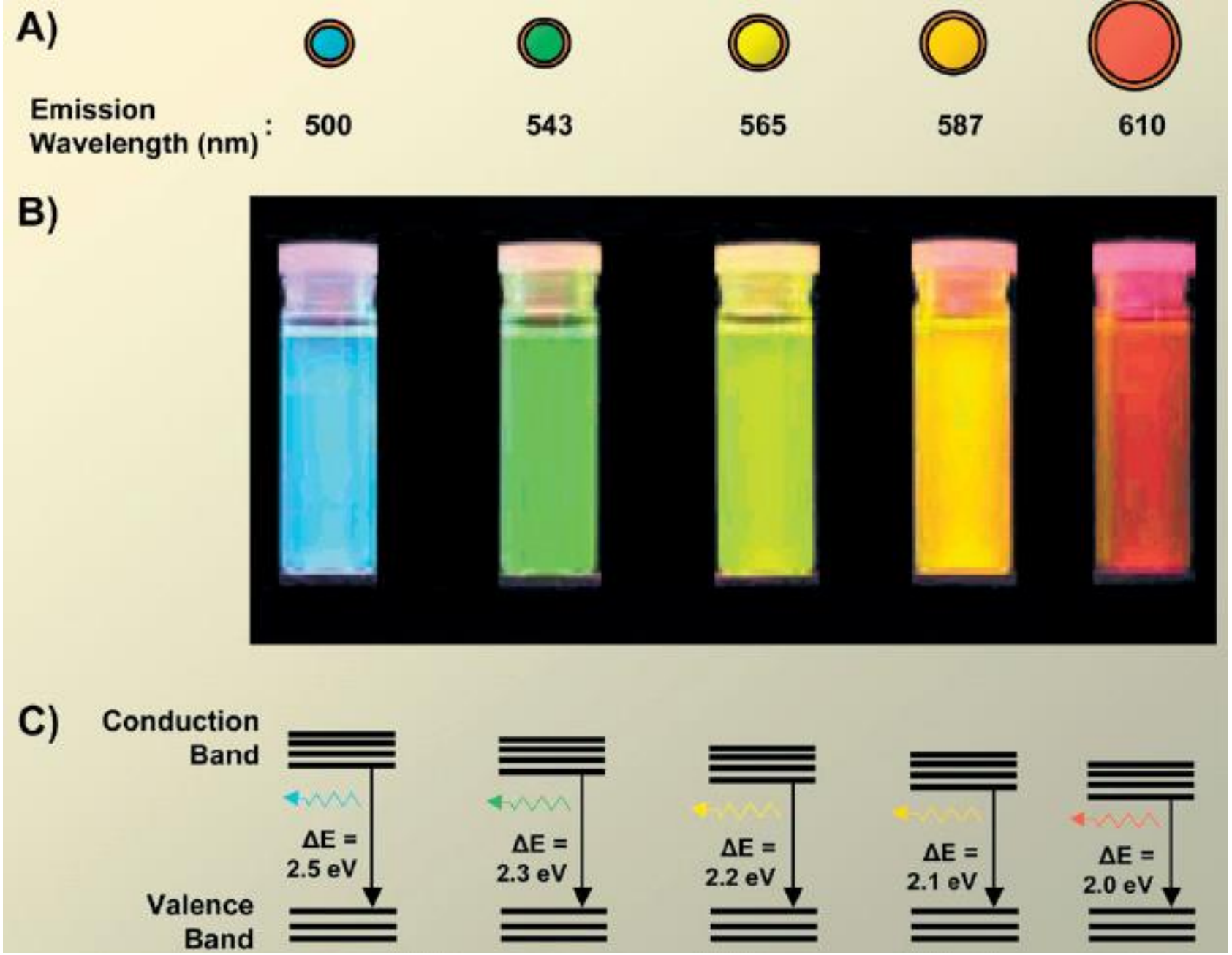

J. M. Klostranec, W. C. W. Chan, *Adv. Mater.* **2006**, *18*, 1953.

Representative QD core materials scaled as a function of their emission wavelength superimposed over the spectrum. Representative areas of biological interest

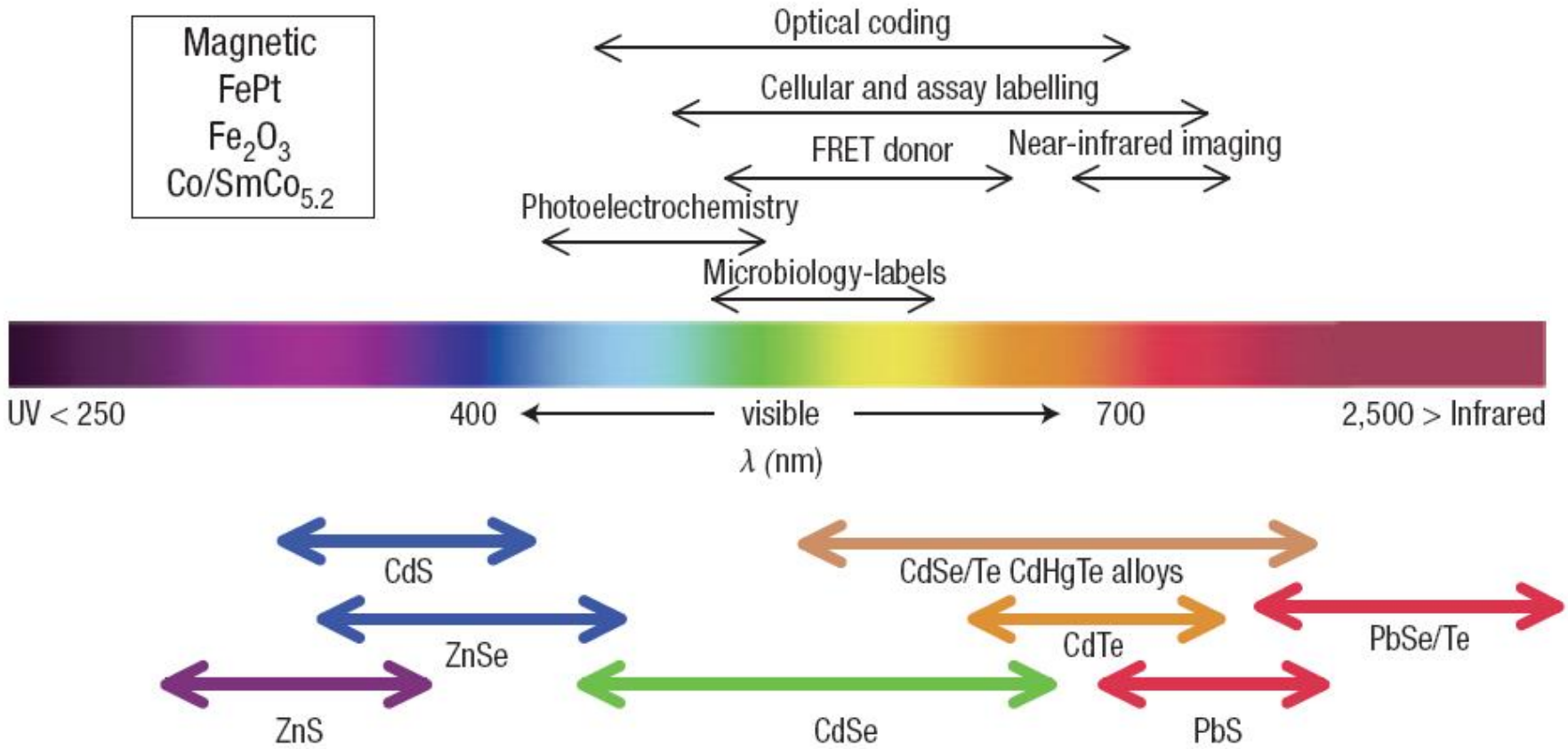

Pseudo-colored image depicting five-color QD staining of fixed human epithelial cells.

Cyan corresponds to 655-nm Qdots labelling the nucleus,
magenta 605-Qdots labelling Ki-67 protein,
orange 525-Qdots labelling mitochondria,
green 565-Qdots labelling microtubules
and red 705-Qdots labelling actin filaments.

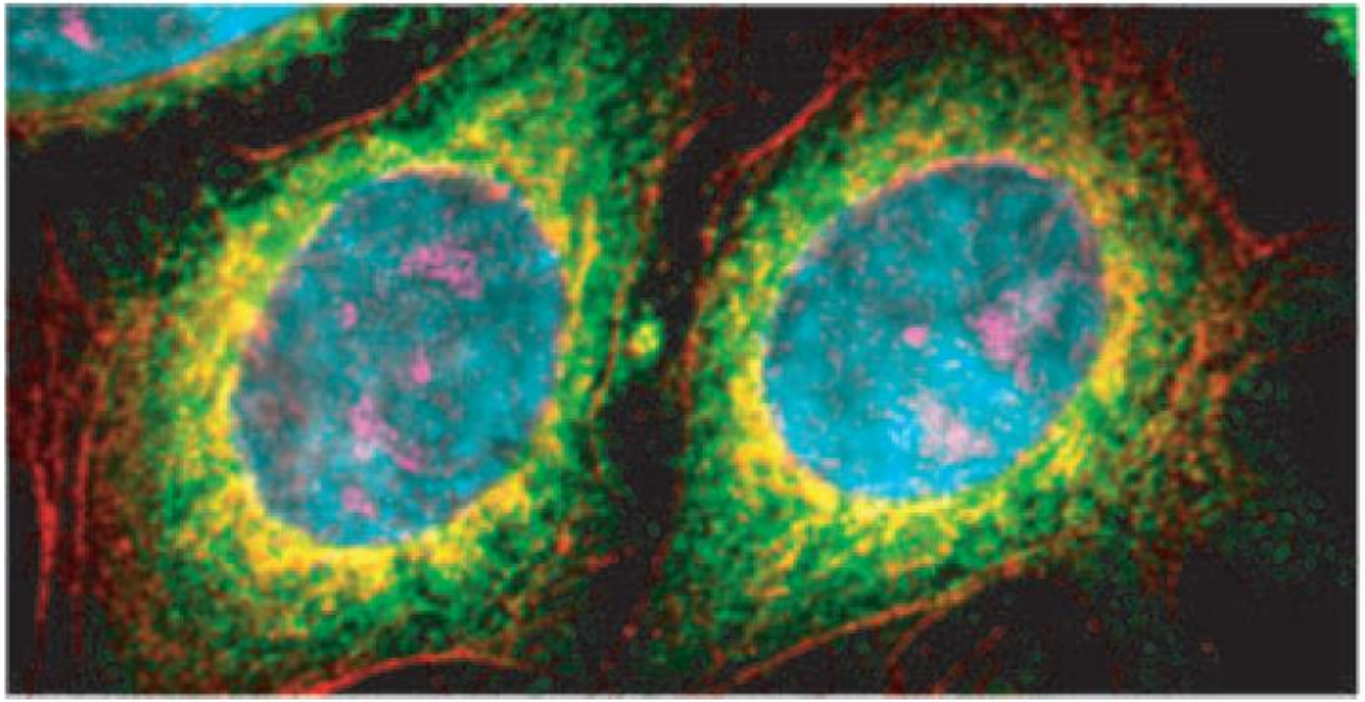

Fluorescent Bio-imaging using QDs

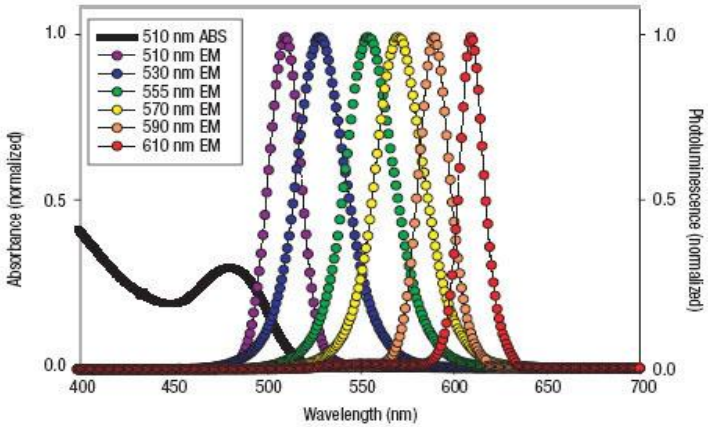

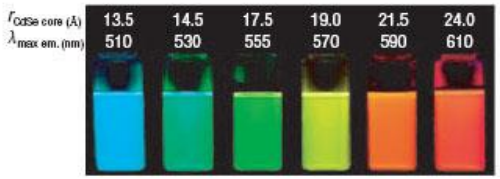

Medintz et. al. , *Nat. Mater.* **2005,** *4*, 435.

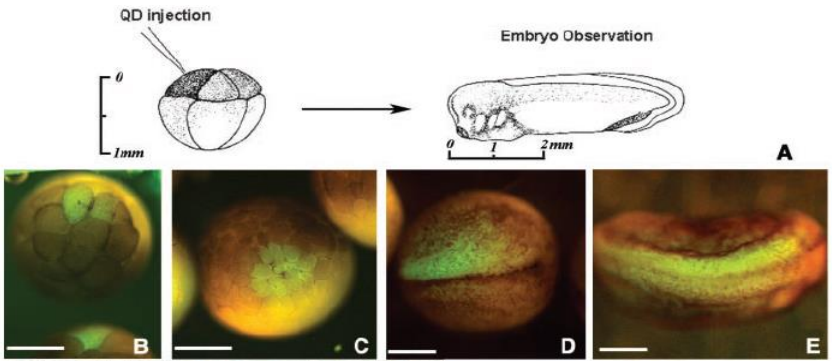

Dubertret et. al., *Science* **2002**, *298*, 1759.

Differentiation of *Xenopus* embryos to cells

Advantage

- **Long term stability**
- **Various wavelength**
- **Narrow emission**

Limitation

- **Highly toxic cadmium**
- **Shallow penetration depth to living organ**

Water-dispersible Nanoparticles

Hydrophobic shell

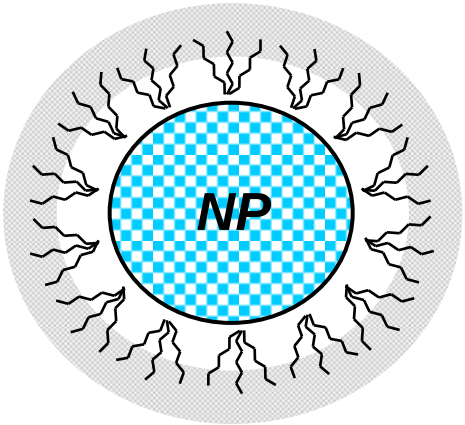

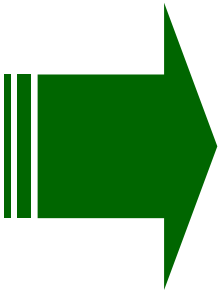

Ligand Exchange with hydrophilic ligands

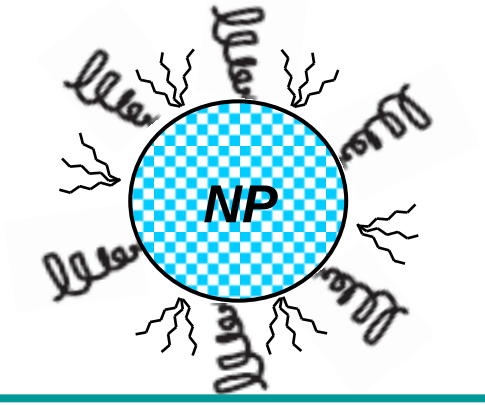

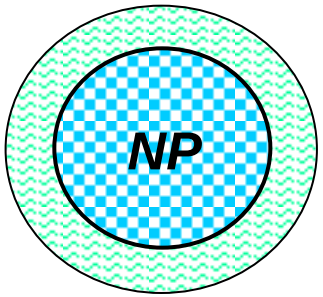

Encapsulation with hydrophilic surface

QD solubilization and biofunctionalization

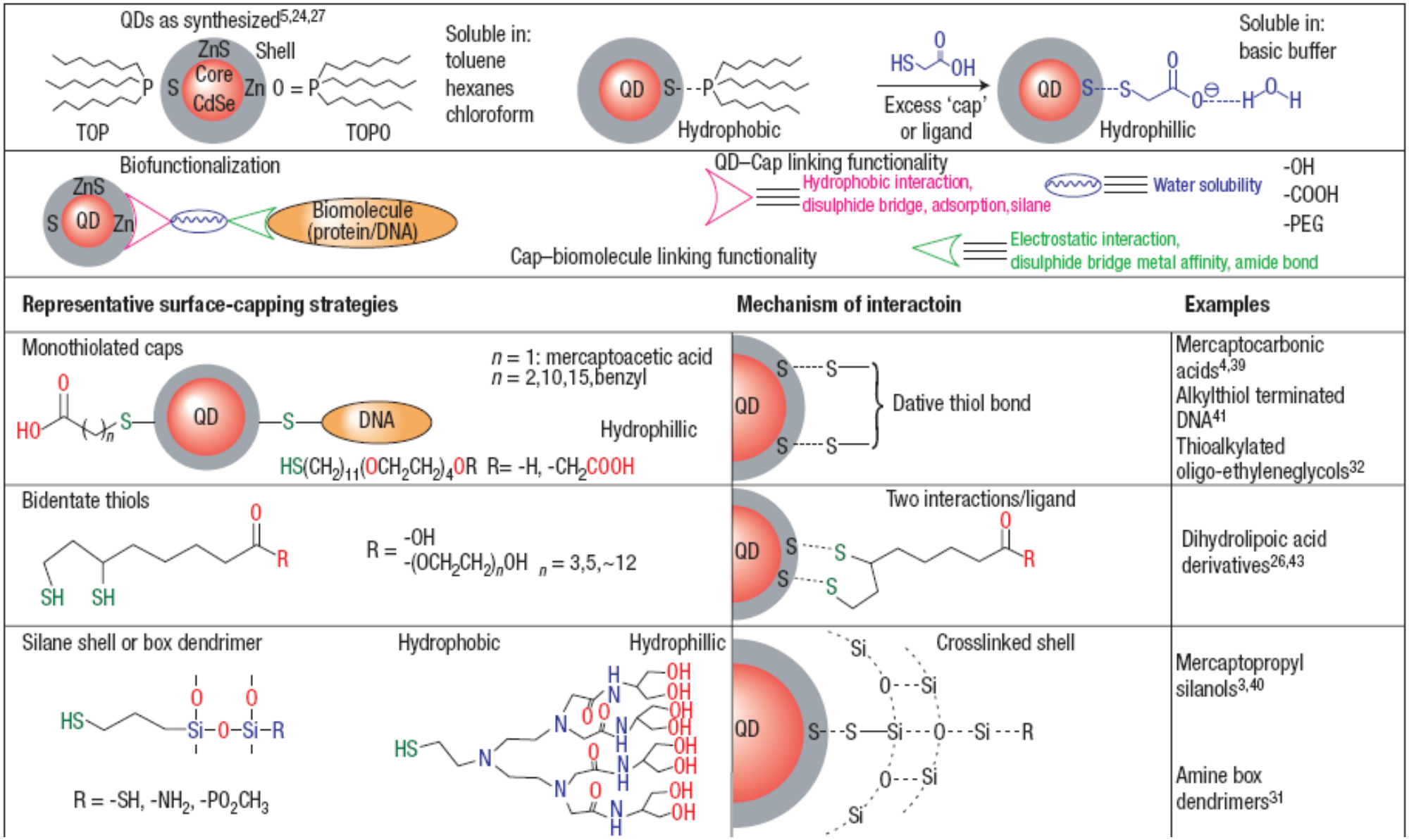

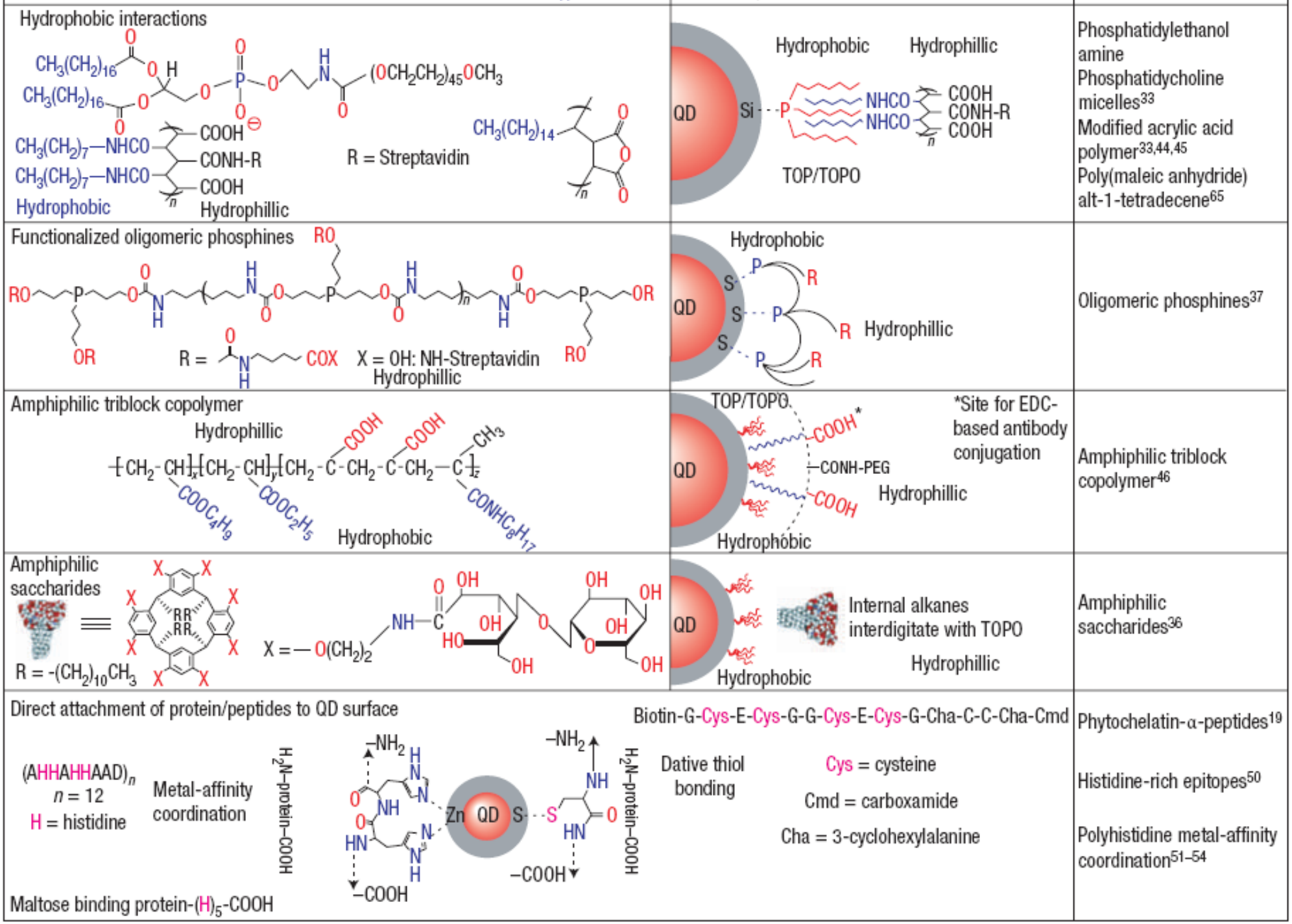
d
Hydrophobic interactions
R = Streptavidin
Hydrophobic
Hydrophillic
QD
Hydrophobic
Hydrophillic
TOP/TOPO
Phosphatidylethanol amine
Phosphatidycholine micelles33
Modified acrylic acid polymer33,44,45
Poly(maleic anhydride) alt-1-tetradecene65
e
Functionalized oligomeric phosphines
R = COX
X = OH: NH-Streptavidin
Hydrophillic
QD
Hydrophobic
Hydrophillic
Oligomeric phosphines37
f
Amphiphilic triblock copolymer
Hydrophillic
Hydrophobic
TOP/TOPO
*Site for EDC-based antibody conjugation
QD
Hydrophillic
Hydrophobic
Amphiphilic triblock copolymer46
g
Amphiphilic saccharides
R = -(CH2)10CH3
X = —O(CH2)2
QD
Internal alkanes interdigitate with TOPO
Hydrophobic
Hydrophillic
Amphiphilic saccharides36
h
Direct attachment of protein/peptides to QD surface
Biotin-G-Cys-E-Cys-G-G-Cys-E-Cys-G-Cha-C-C-Cha-Cmd
Phytochelatin-α-peptides19
(AHHAHHAAD)n
n = 12
H = histidine
Metal-affinity coordination
H2N–protein–COOH
Zn QD S
Dative thiol bonding
Cys = cysteine
Cmd = carboxamide
Cha = 3-cyclohexylalanine
Histidine-rich epitopes50
Polyhistidine metal-affinity coordination51–54
Maltose binding protein-(H)5-COOH

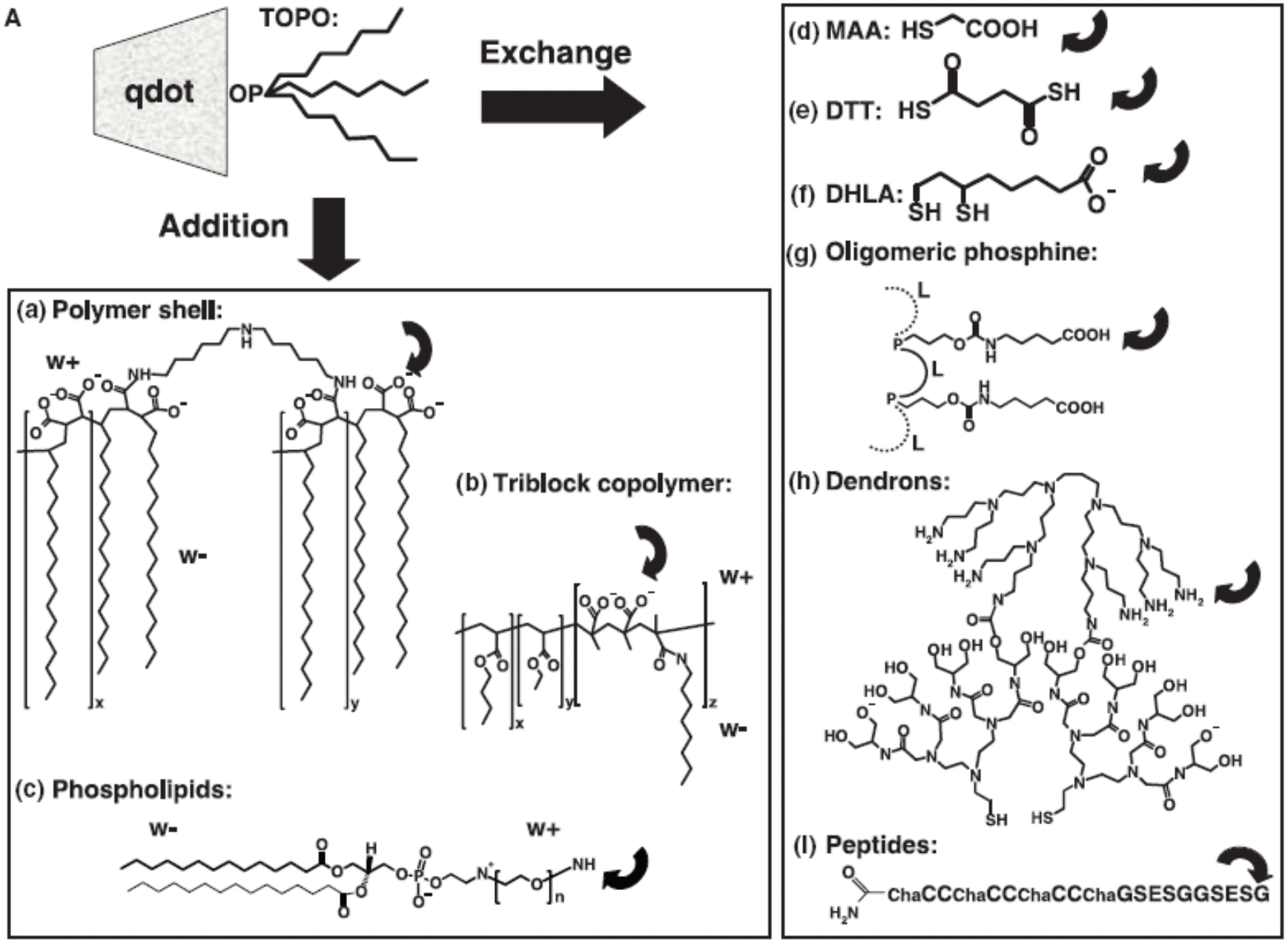

X. Michalet, …….. S. S. Gambhir, S. Weiss, *Science* **2005**, *307*, 538

Schematic of current Qdot surface coatings

Jesse M. Klostranec and Warren C. W. Chan* *Adv. Mater.* **2006**, 18, 1953.

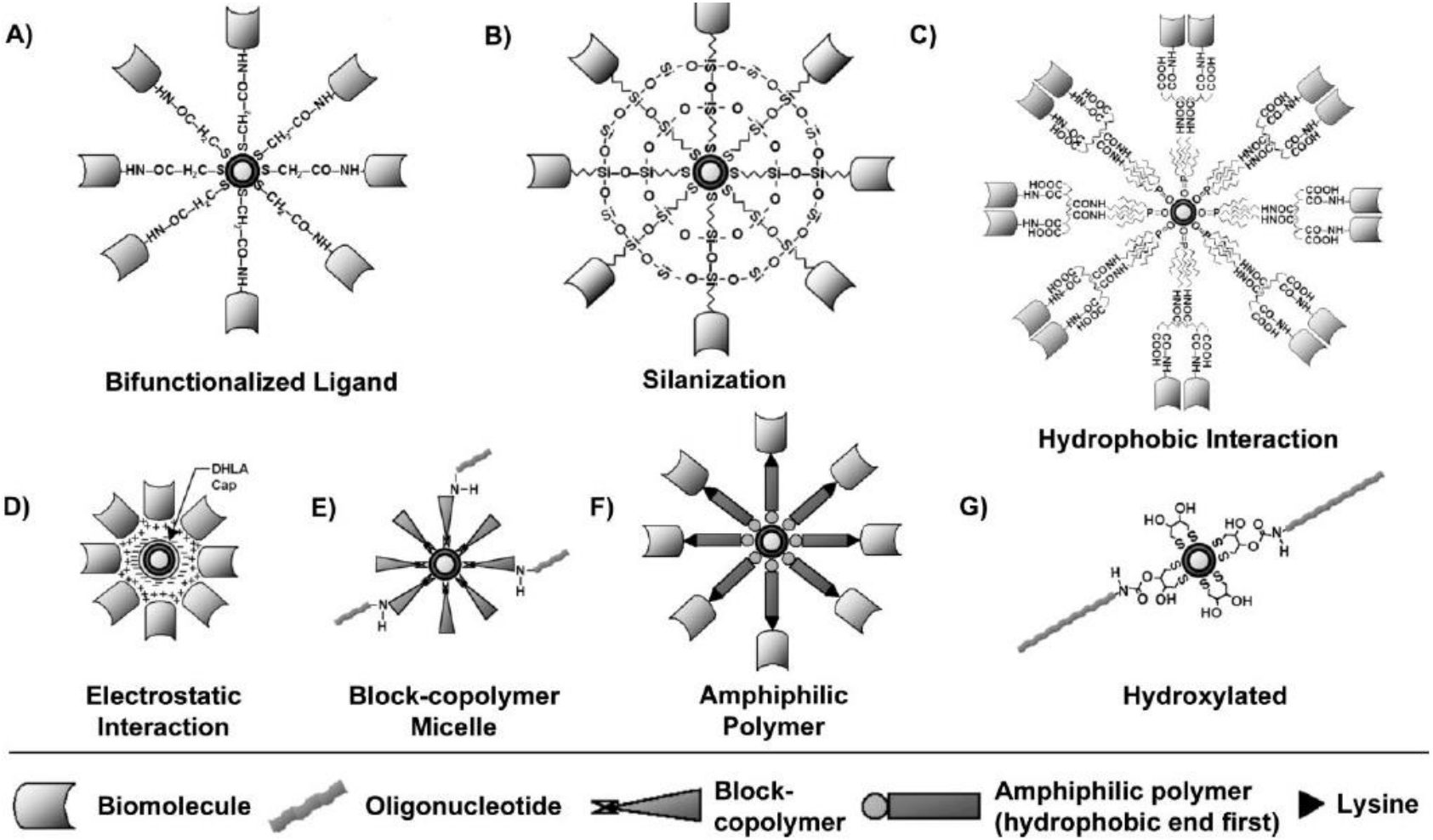

A) bifunctionalization, B) silanization, C) hydrophobic–hydrophobic interaction, D) electrostatic interaction, E) micelle encapsulation, F) amphiphilic polymer, G) hydroxylation.

Semiconductor Nanocrystals as Fluorescent Biological Labels

Shimon Weiss and A. Paul Alivisatos (U. California, Berkeley)

Science **1999**, 281, 2013.

The use of nanocrystals for biological detection.

A. Paul Alivisatos, *Nature Biotechnology* **2004**, 22, 47.

Demonstration of Photostability of QD's vs conventional dye

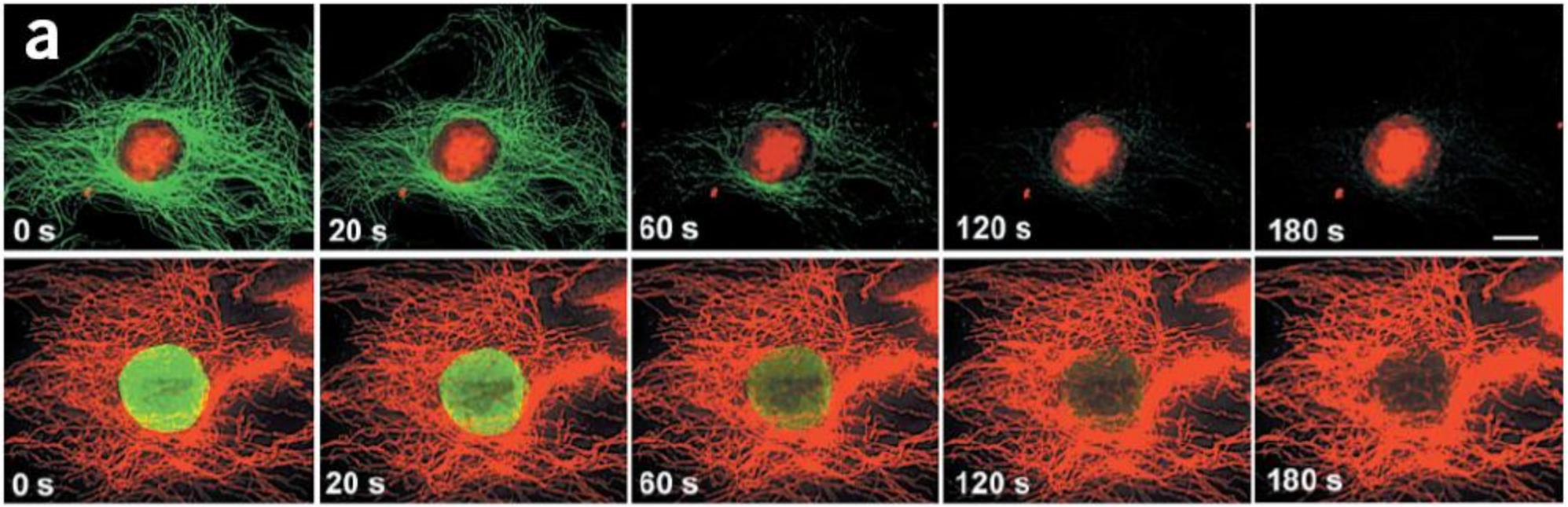

Advantages of QDs over conventional dyes for Biological imaging

1. Semiconductor nanocrystals were prepared for use as fluorescent probes in biological staining and diagnostics.
2. Compared with conventional fluorophores, the nanocrystals have a narrow, tunable, symmetric emission spectrum and are photochemically stable.
3. The advantages of the broad, continuous excitation spectrum were demonstrated in a dual-emission, single-excitation labeling experiment on mouse fibroblasts: Many sizes of nanocrystals may therefore be excited with a single wavelength of light; many emission colors that may be detected simultaneously.
4. These nanocrystal probes are thus complementary and in some cases may be superior to existing fluorophores.

Excitation (dashed) and fluorescence (solid) spectra of (**A**) fluorescein and (**B**) a typical water-soluble nanocrystal (NC)

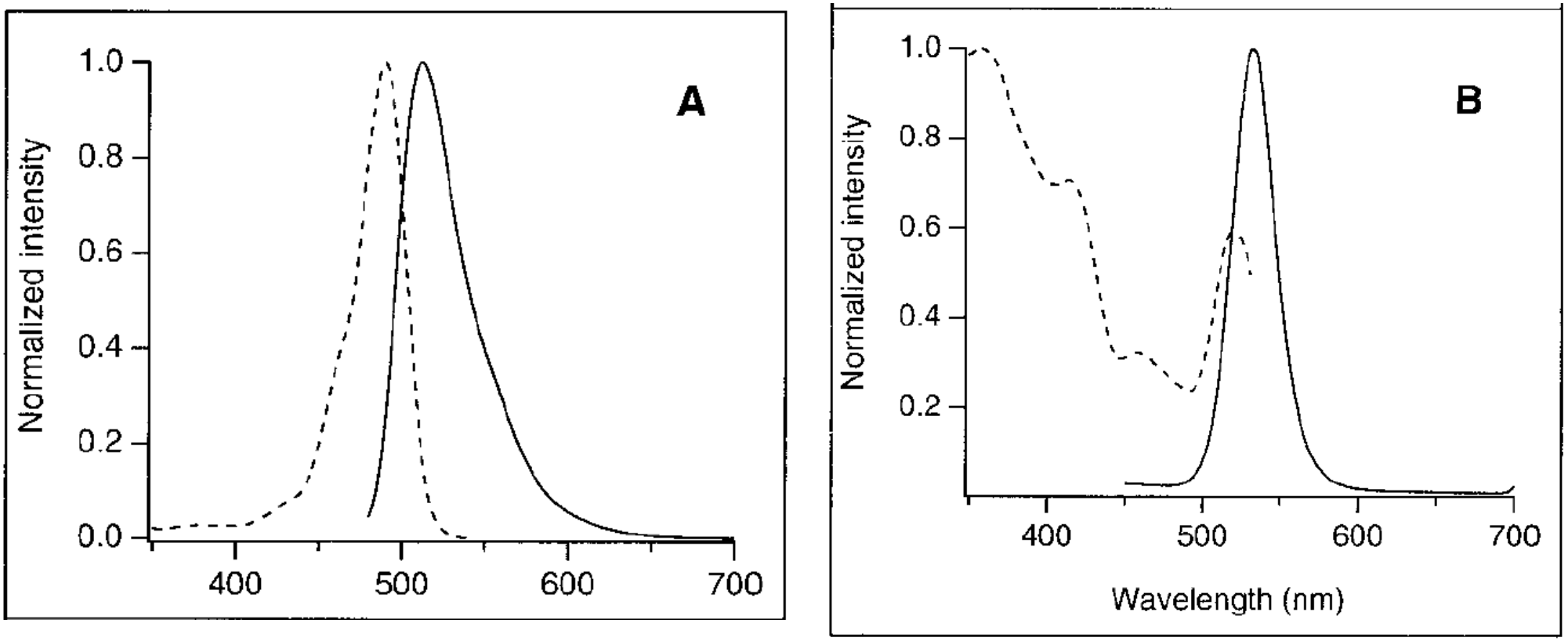

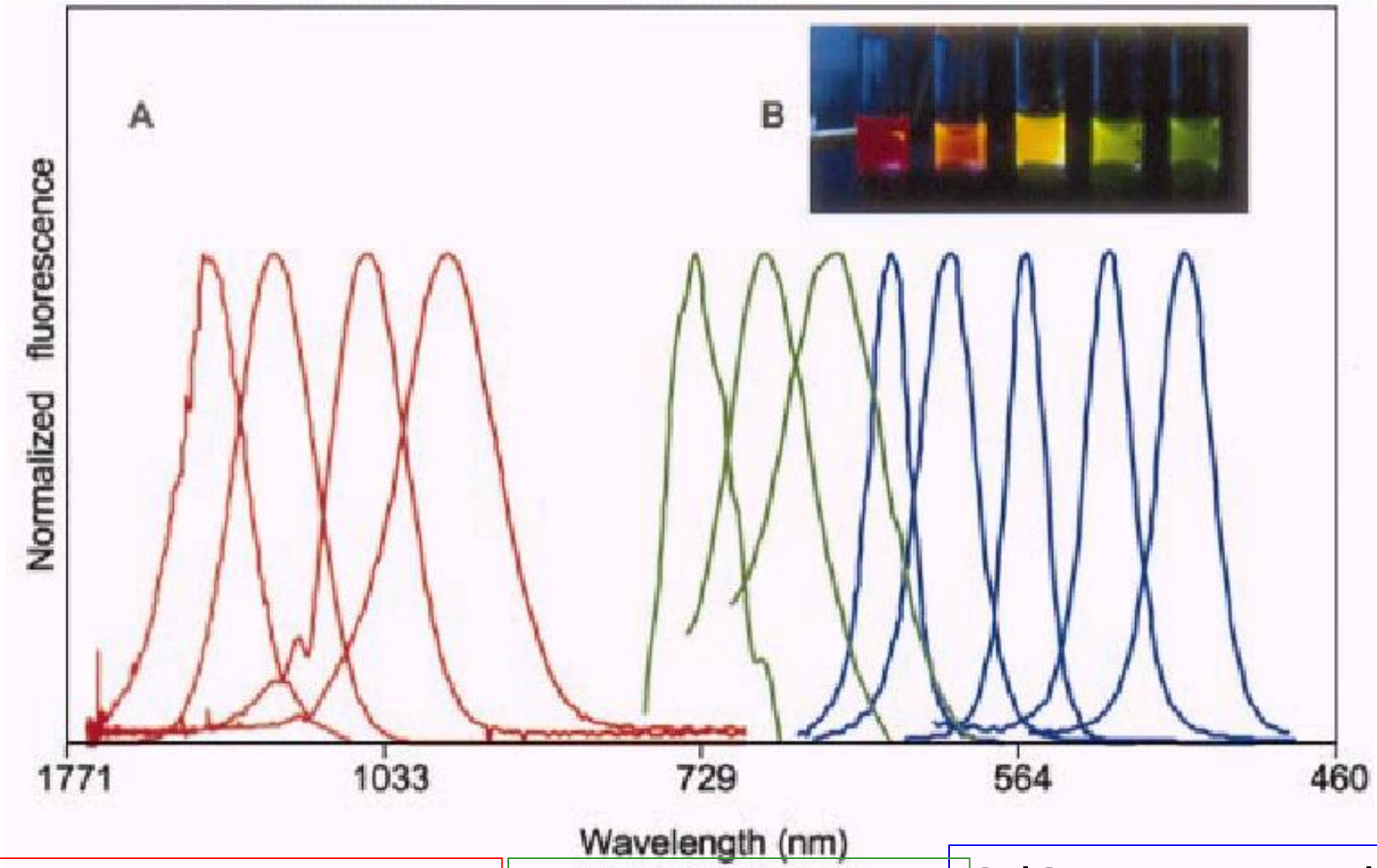

InAs nanocrystals
2.8, 3.6, 4.6, and 6.0 nm

InP nanocrystals
3.0, 3.5, and 4.6 nm

CdSe nanocrystals 2.1, 2
3.1, 3.6, and 4.6 nm

B: silica-coated core (CdSe)–shell (ZnS or CdS) nanocrystal probes

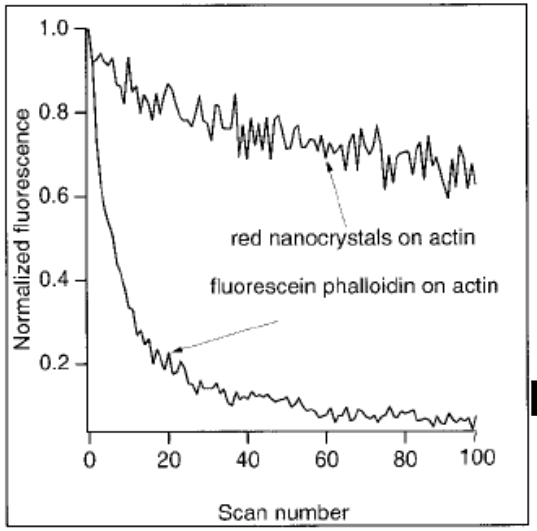

Sequential scan photostability comparison

- Cross section of a dual-labeled sample examined with a Bio-Rad 1024 MRC laser-scanning confocal microscope.
- 3T3 mouse fibroblast cells using two different size CdSe-CdS core-shell nanocrystals enclosed in a silica shell.
- The smaller nanocrystals (2-nm core) emitted green fluorescence (maximum 550 nm, 15% quantum yield), the larger (4-nm core), red fluorescence (maximum 630 nm, 6% quantum yield)

• nanocrystals coated with trimethoxysilylpropyl urea and acetate groups were found to bind with high affinity in the cell nucleus

→ "stain" the nucleus with the green-colored nanocrystals,

• Avidin-biotin interaction: a model Biotin was covalently bound to the nanocrystal surface, and the biotinylated nanocrystals were used to label fibroblasts. Fibroblasts had been incubated in phalloidin-biotin.

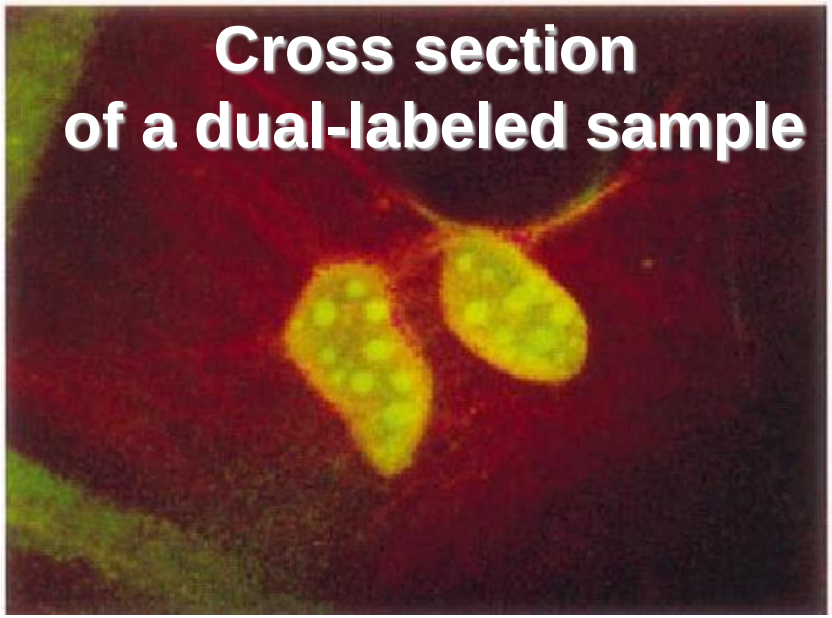

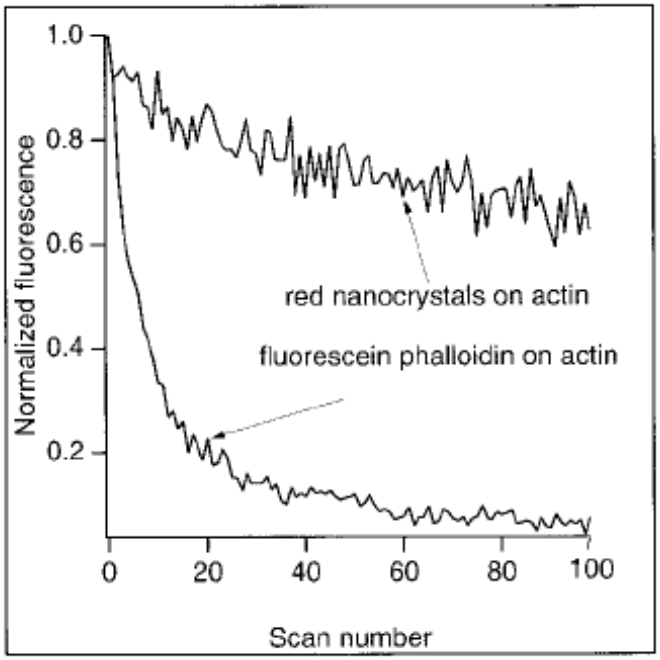

Sequential scan photostability comparison

Quantum Dot Bioconjugates for Ultrasensitive Nonisotopic Detection

Warren C. W. Chan and Shuming Nie*

Science **1998**, 281, 2016.

Mercaptoacetic acid

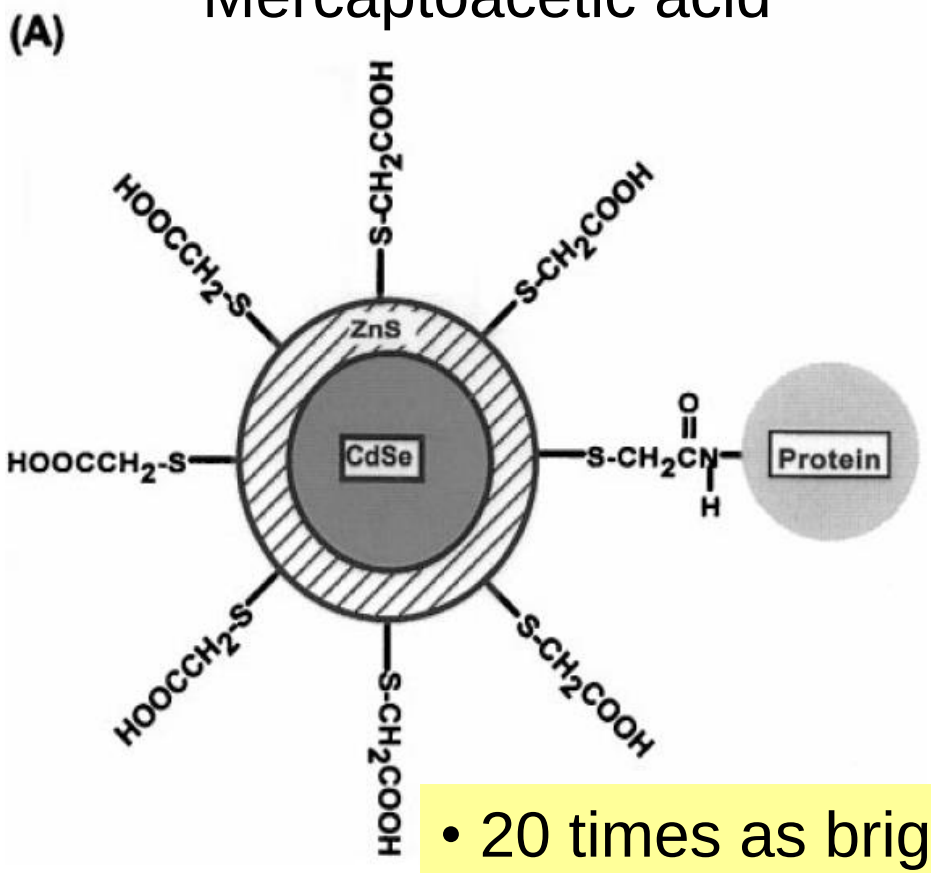

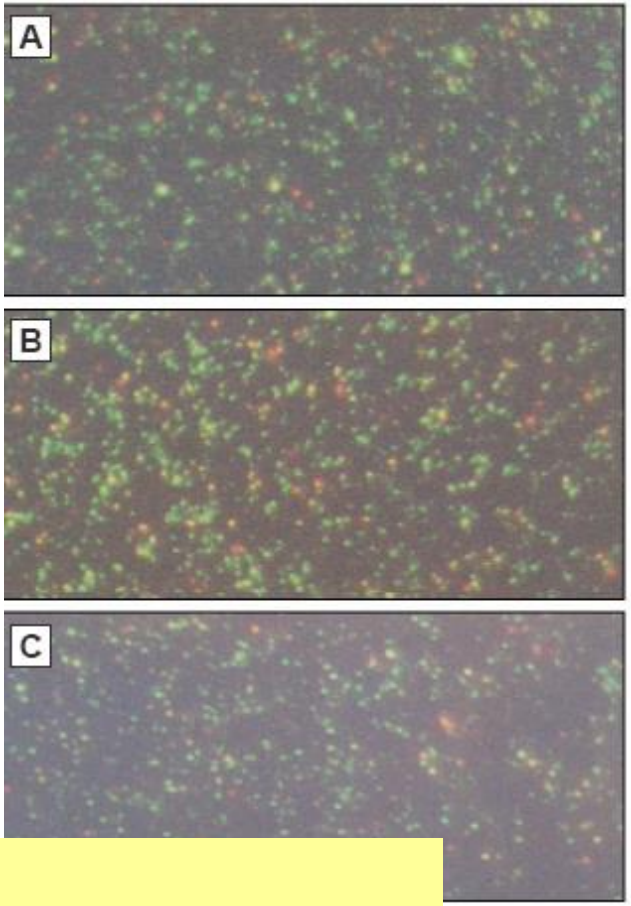

- 20 times as bright
- 100 times as stable against photobleaching
- one-third as wide in spectral linewidth.

Biomolecule-Nanocrystal Conjugate

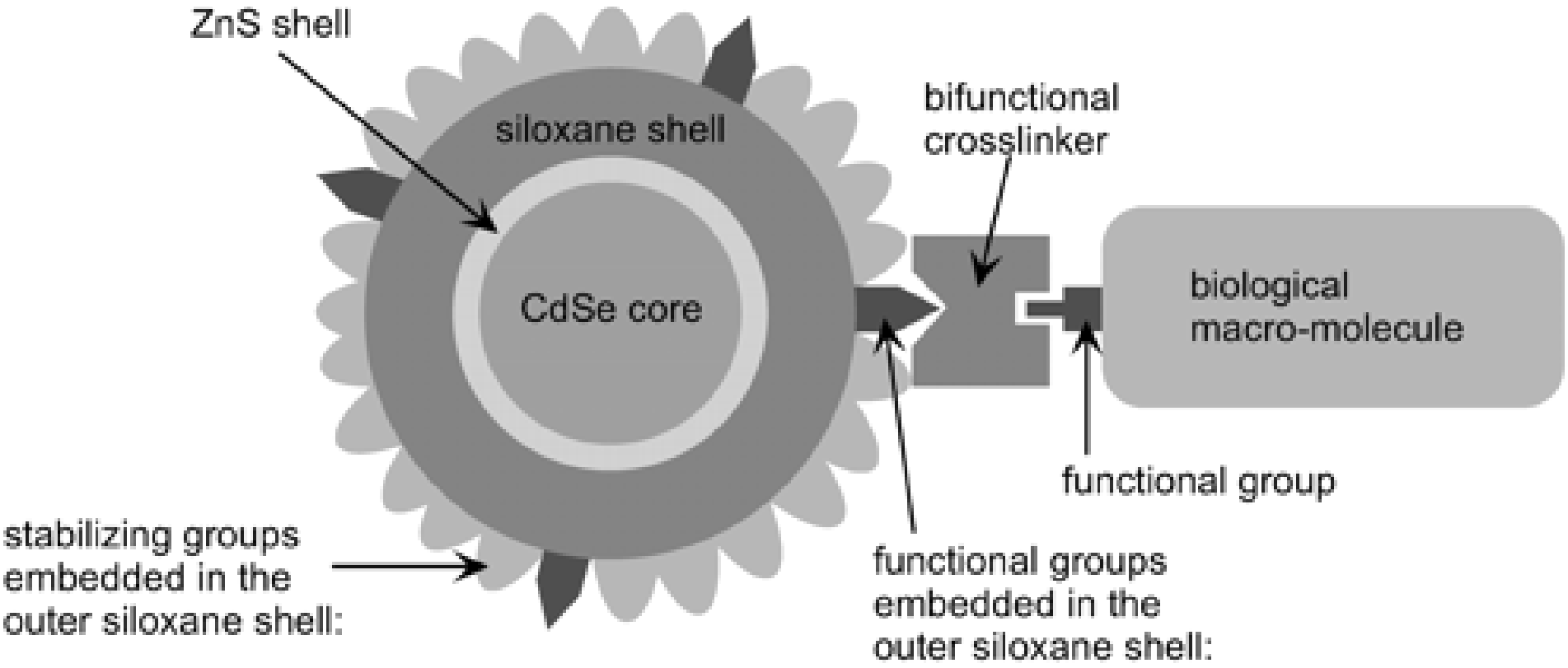

CdSe/ZnS core/shell nanocrystals

Near-infrared fluorescent type II quantum dots for sentinel lymph node mapping,

Sungjee Kim, Yong Taik Lim, ……., M. G. Bawendi, J. H. Frangioni,

Nature Biotechnology **2004**, 22, 93.

- Fluorescence emission of type II quantum dots can be tuned into the near infrared and that a polydentate phosphine coating renders them soluble, disperse and stable in serum.
- Type II NIR QDs with a hydrodynamic diameter of 15–20 nm, a maximal absorption cross-section, fluorescence at 840–860 nm
- NIR QD size of 16 nm = 440 kDa protein → critical diameter of 5 ~ 50 nm needed for retention of QDs in sentinel lymph node (SLN)

Sentinel lymph node:

First lymph node(s) reached by metastasizing cancer cells from a tumor.

• By changing the two variables of shell thickness and core size, the emission of type-II QDs can be easily and widely tuned.

• PL spectra from CdTe/CdSe QDs that range from 700 nm to over 1000 nm simply by changing the core size and shell thickness.

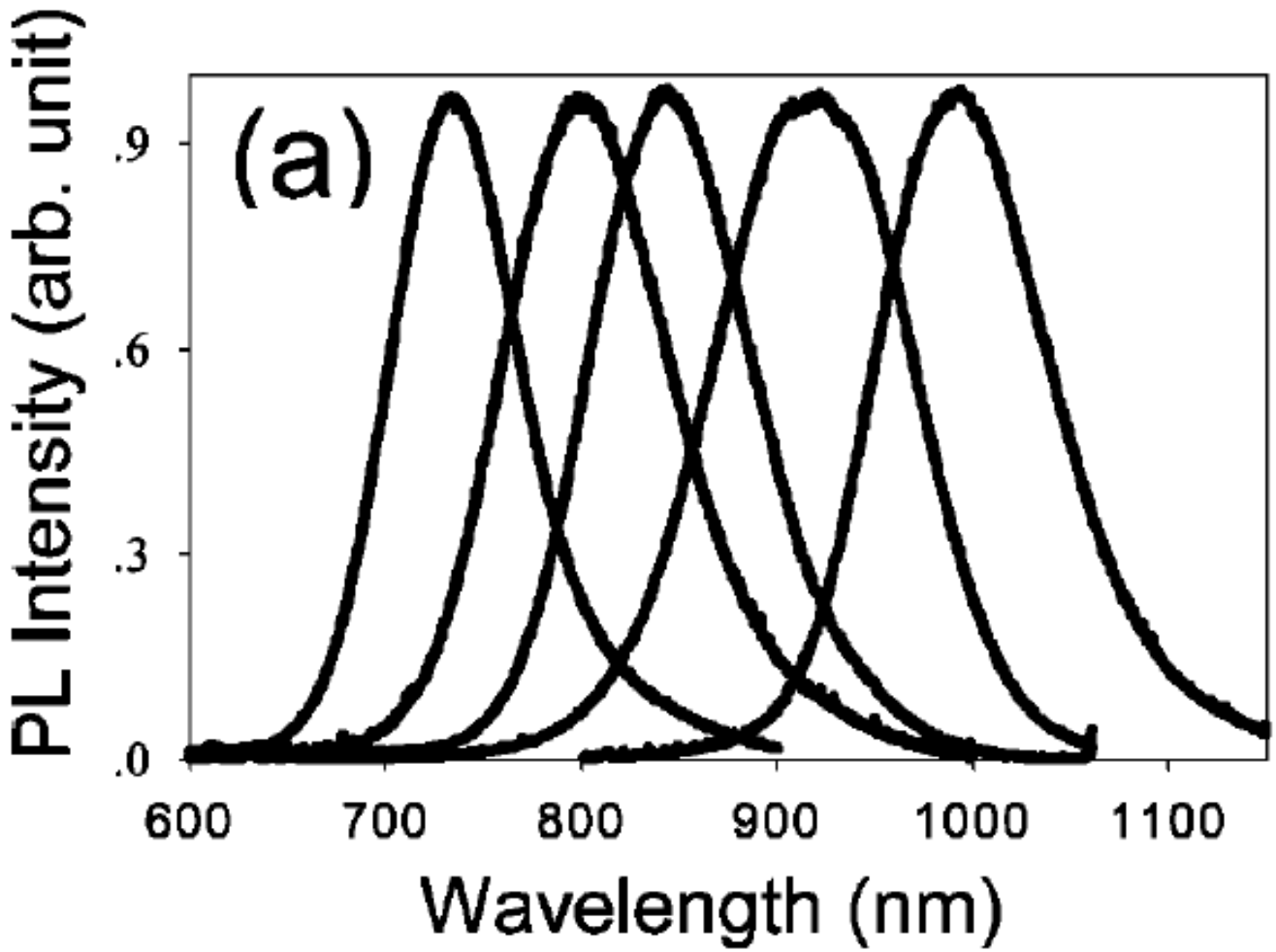

NIR emitting window is appealing for biological optical imaging because of the low tissue absorption and scattering effects. typically at 650–900 nm

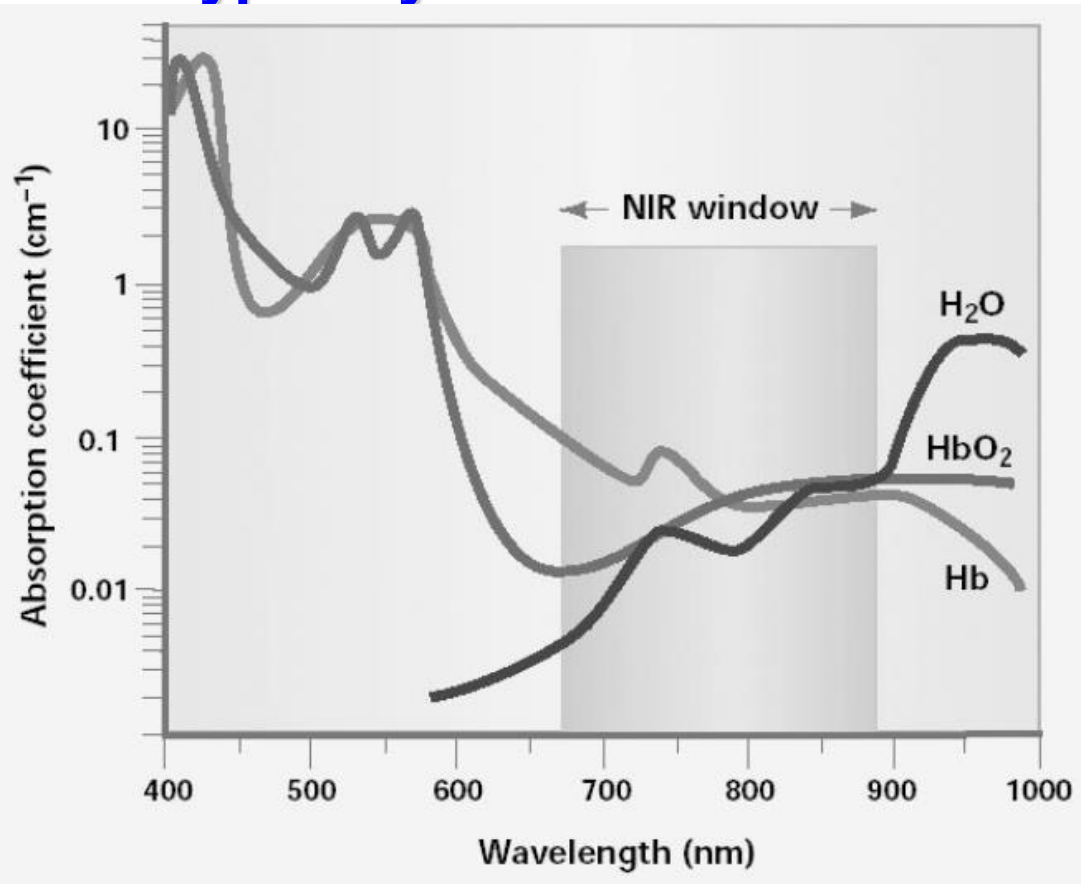

R. Weissleder, *Nature Biotechnol.* **2001**, *19*, 316.

- Demonstrate that these quantum dots allow a major cancer surgery, sentinel lymph node mapping, under complete image guidance.
- Injection of only 400 pmol of near-infrared quantum dots permits sentinel lymph nodes 1 cm deep to be imaged easily in real time using excitation fluence rates of only 5 mW/cm^2.
- Localization of SLN → only 3 -4 min
- Image guidance using NIR QDs minimized size of incision to find node

Sentinel lymph node:
First lymph node(s) reached by metastasizing cancer cells from a tumor.

NIR QD sentinel lymph node mapping in the mouse

Images of mouse injected intradermally with 10 pmol of NIR QDs in the left paw.

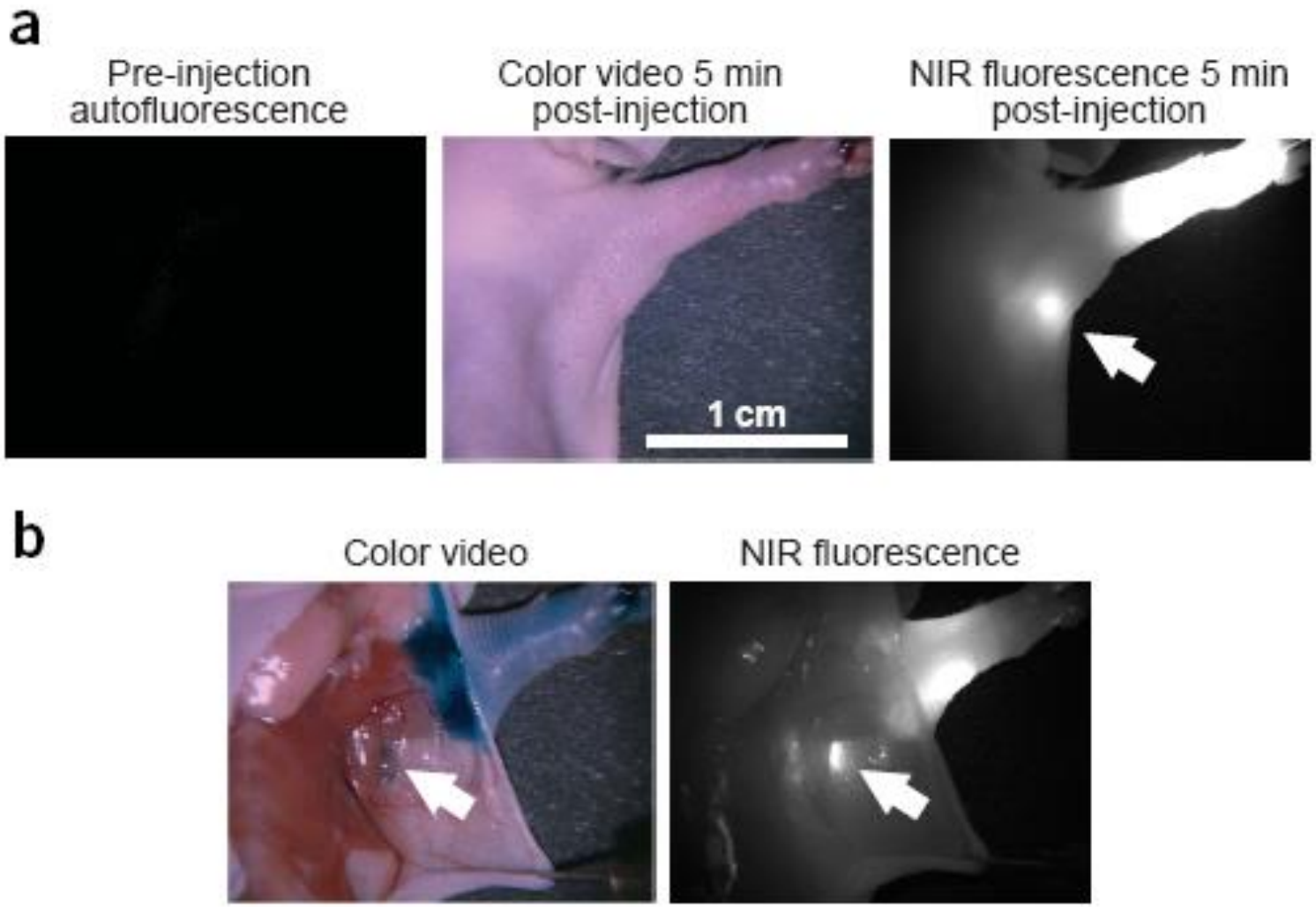

Sentinel lymph node:
First lymph node(s) reached by metastasizing cancer cells from a tumor.

Surgical field in a pig injected intradermally with 400 pmol of NIR QDs in the right groin.

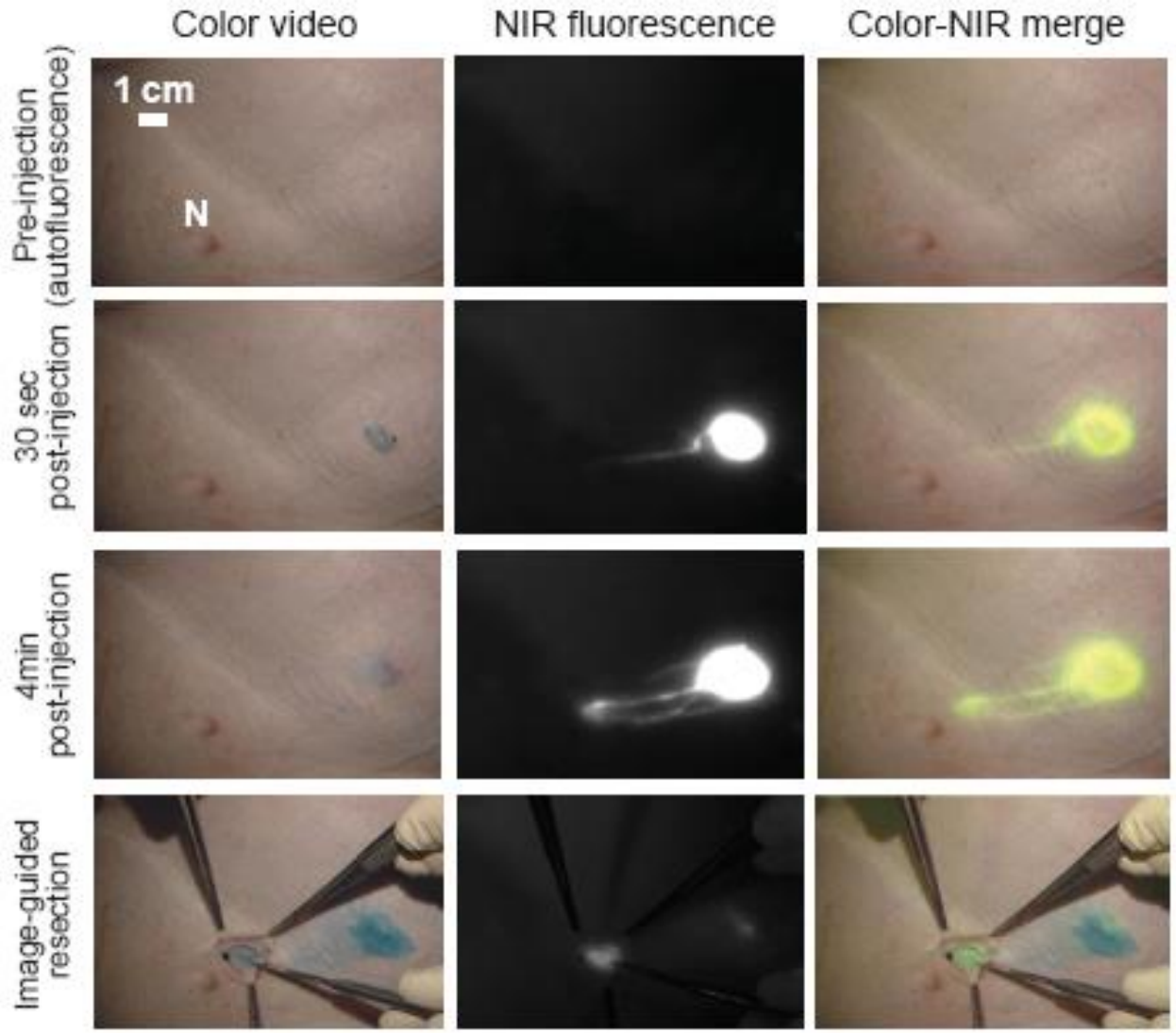

In Vivo Imaging of Quantum Dots Encapsulated in Phospholipid Micelles

Benoit Dubertret,1,3*† Paris Skourides,2 David J. Norris,3,4*
Vincent Noireaux,1 Ali H. Brivanlou,2 Albert Libchaber1,3

Science **2002**, 298, 1759.

- Encapsulation of individual nanocrystals in phospholipid block–copolymer micelles
- When conjugated to DNA, the nanocrystal-micelles acted as in vitro fluorescent probes to hybridize to specific complementary sequences.
- Moreover, when injected into *Xenopus* embryos, the nanocrystal-micelles were stable, nontoxic (5 x 10^9 nanocrystals per cell), cell autonomous, and slow to photobleach.
- Nanocrystal fluorescence could be followed to the tadpole stage, allowing lineage-tracing experiments in embryogenesis.

QD-micelle formation

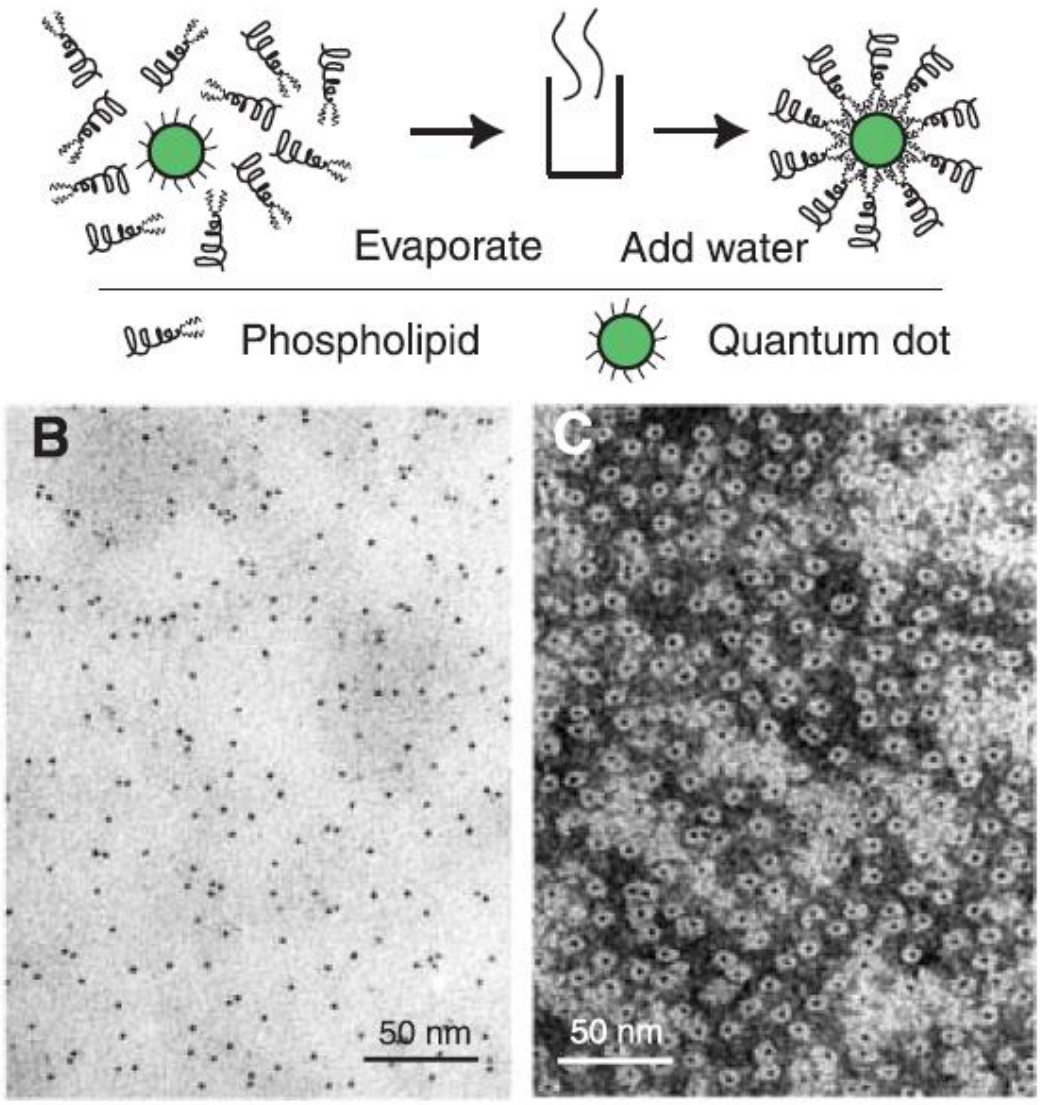

Water-dispersible Nanoparticles

Hydrophobic shell

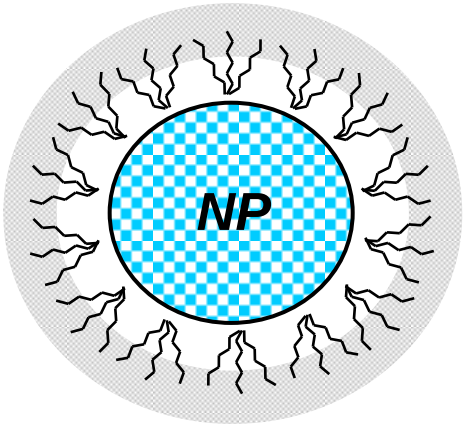

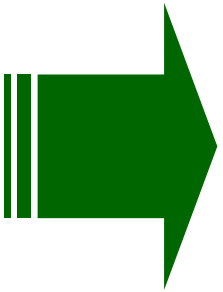

Ligand Exchange with hydrophilic ligands

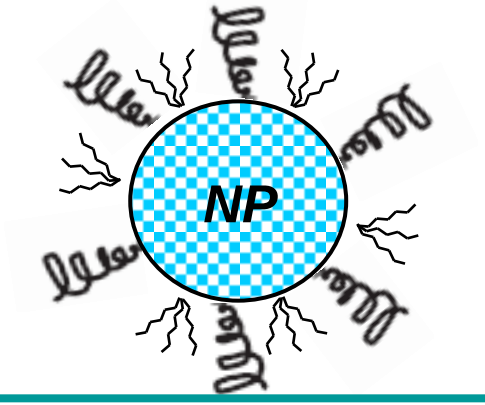

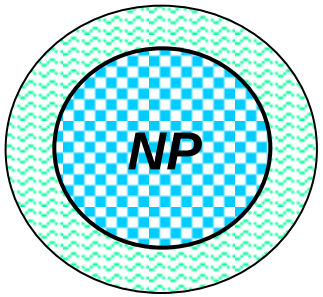

Encapsulation with hydrophilic surface

Conjugation of QD-micelles with DNA.

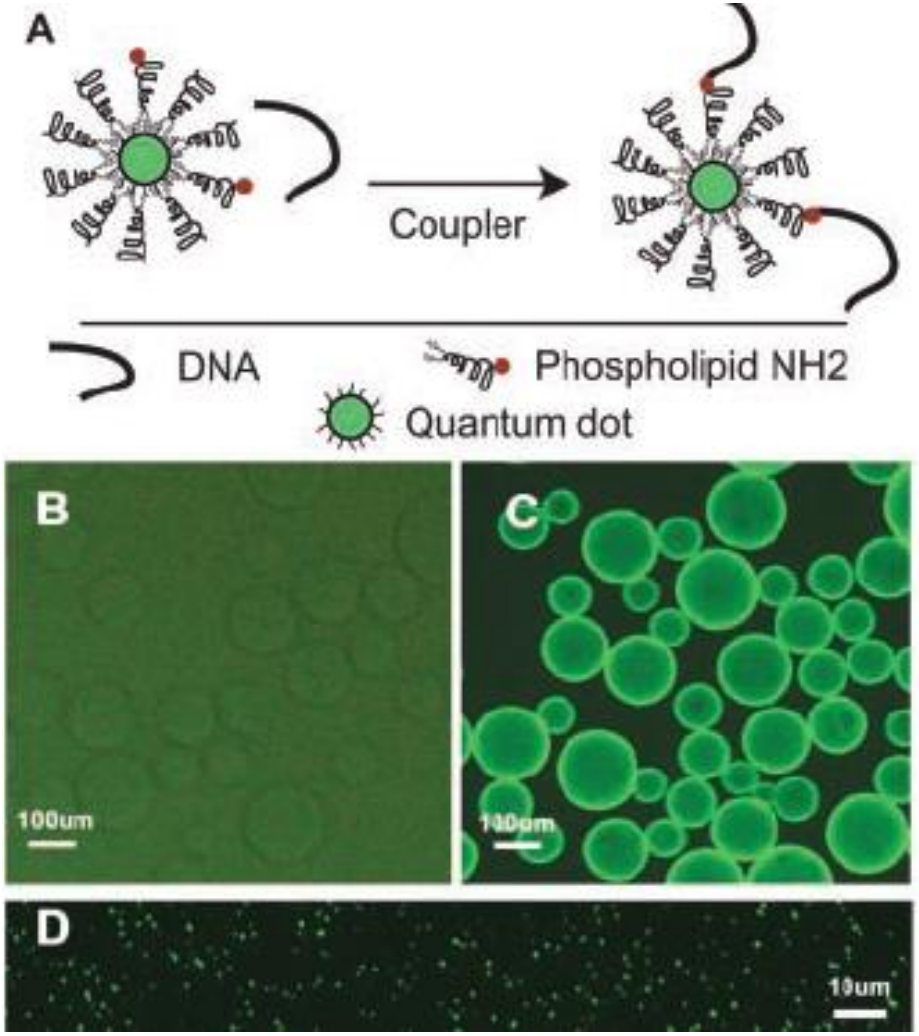

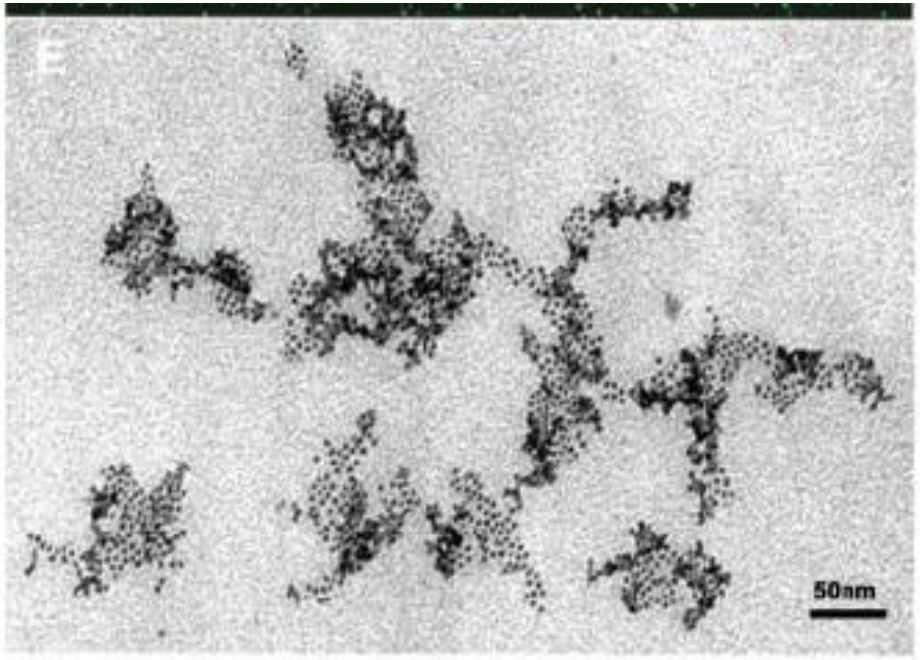

Oligonucleotide–QD-micelles were shown to bind specifically to cDNA, immobilized in 4% agarose beads, but not to noncomplementary oligonucleotides

QD labeling of Xenopus embryos at different stages: Real-time tracking of embryonic development

Requirements for in vivo imaging

- **Biologically neutral (i.e., no biological activity or toxicity).**
- **Stable for long periods of time**

Important for cell tracking

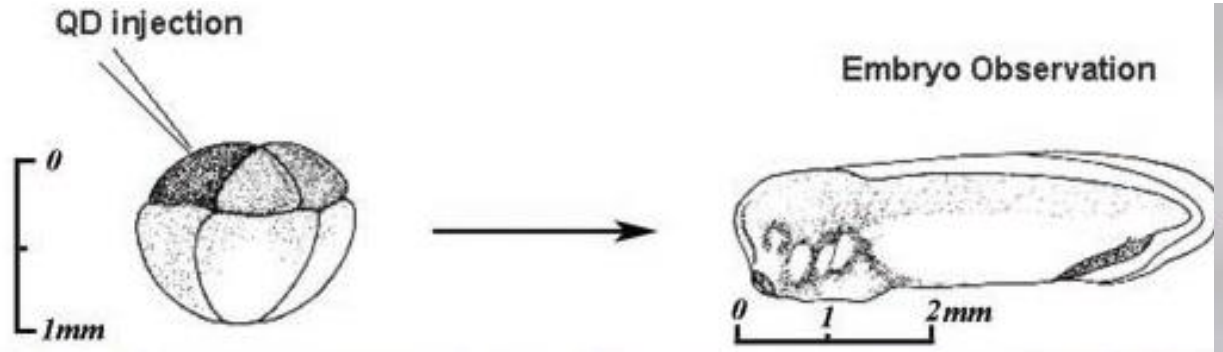

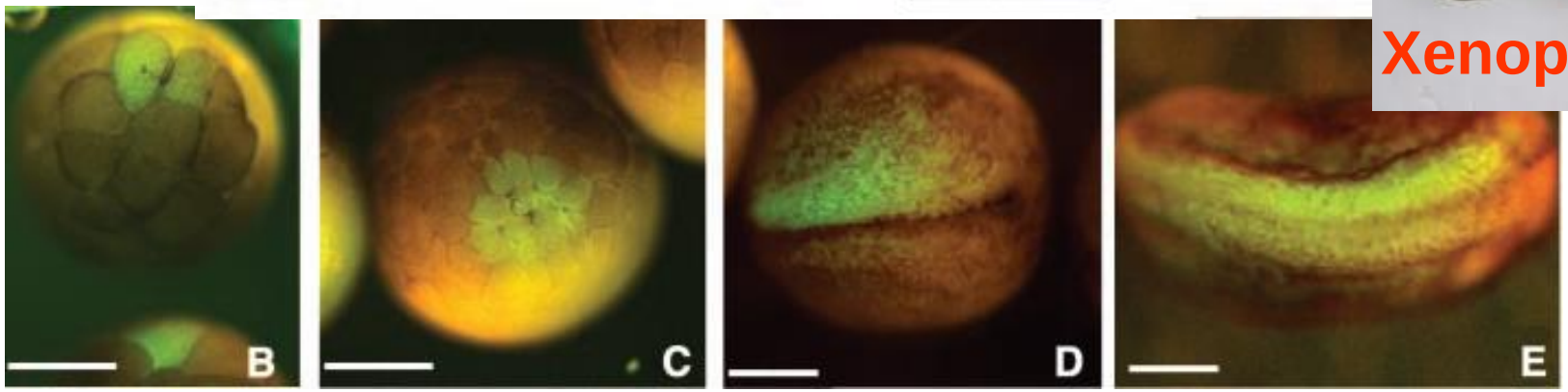

- **QD-micelles were cell autonomous.**
- **QD-micelles seemed to have very little activity or toxicity.**
- **QD-micelles were stable in vivo.**

Comparison of QD and RG-D (Rhodamine Green Dextran) for resistance to photobleaching.

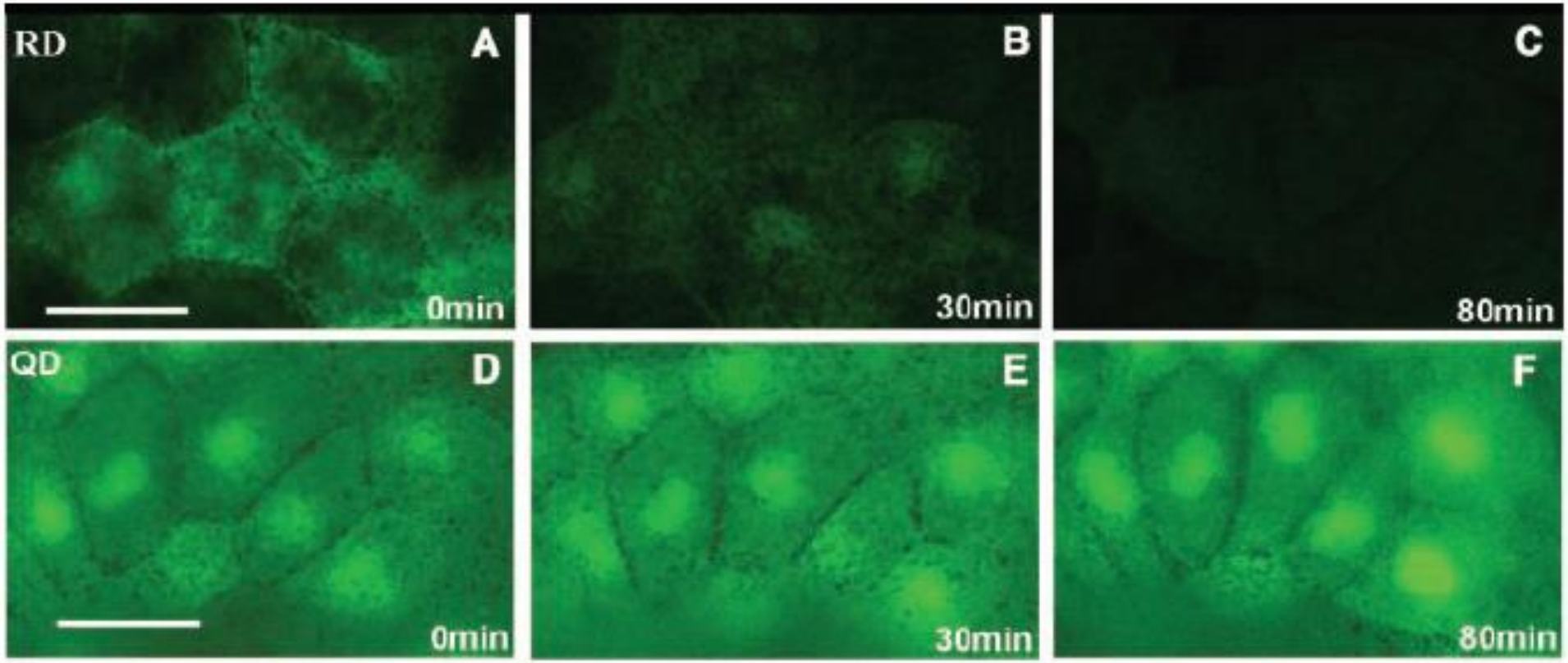

Renal clearance of quantum dots,

H. S. Choi, ……., M. G. Bawendi, J. H. Frangioni,

Nature Biotechnology **2007**, 25, 1165.

- size and charge of most nanoparticles preclude their efficient clearance from the body as intact nanoparticles.
- For globular proteins, a hydrodynamic diameter of ~ 5–6 nm is associated with the ability to be cleared rapidly from the body by renal filtration and urinary excretion
- Without such clearance or their biodegradation into biologically benign components, toxicity is potentially amplified and radiological imaging is hindered. Au nanoparticles for CT.
- Using intravenously administered quantum dots in rodents as a model system, we have precisely defined the requirements for renal filtration and urinary excretion of inorganic nanoparticles.

- Zwitterionic (cysteine) or neutral organic coatings prevented adsorption of serum proteins, which otherwise increased hydrodynamic diameter by 415 nm and prevented renal excretion.
- A final hydrodynamic diameter < 5.5 nm resulted in rapid and efficient urinary excretion and elimination of quantum dots from the body.
- This study provides a foundation for the design and development of biologically targeted nanoparticles for biomedical applications.

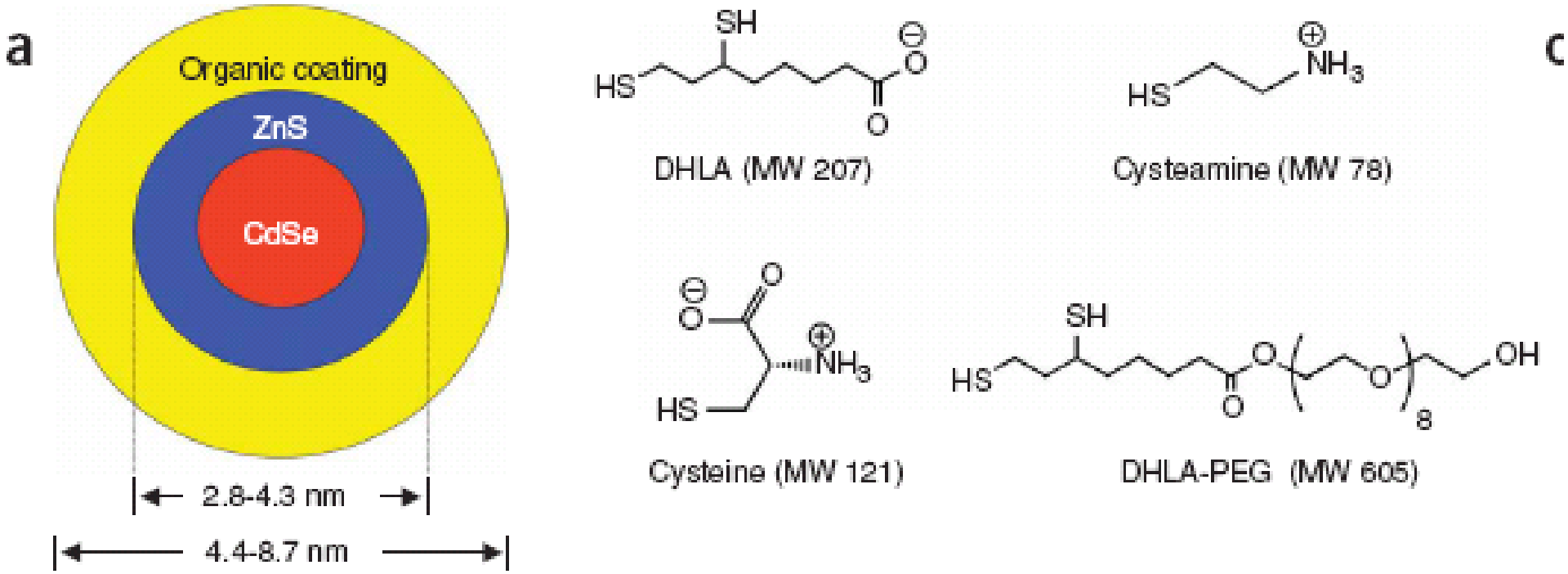

QD-Cys	Em Max (nm)	TEM Diameter (nm)	DLS		GFC
			HD (nm)	%PD	HD (nm)
QD515	515	2.85 ± 0.18	4.64 ± 0.08	20.9	4.36 ± 0.09
QD534	534	3.02 ± 0.20	4.91 ± 0.05	25.9	4.99 ± 0.18
QD554	554	3.30 ± 0.25	5.64 ± 0.01	13.1	5.52 ± 0.14
QD564	574	3.80 ± 0.20	6.40 ± 0.02	24.7	6.70 ± 0.33
QD574	584	4.31 ± 0.46	7.22 ± 0.20	24.8	8.65 ± 0.52

- The larger quantum dots, including DHLA-,cysteamine- and DHLA-PEG–coated ones, were never found in the bladder but, instead, were trapped in the liver, lung and spleen in large amounts
- Four hours after intravenous injection of QD515 (HD = 4.36 nm), the dominant signal was in the bladder.
- In contrast, QD574 (HD = 8.65 nm) exhibited high uptake in liver (26.5 ± 3.9%ID), lung (9.1 ± 4.0%ID) and spleen (6.3 ± 2.4%ID) and a proportionally lower signal in bladder.

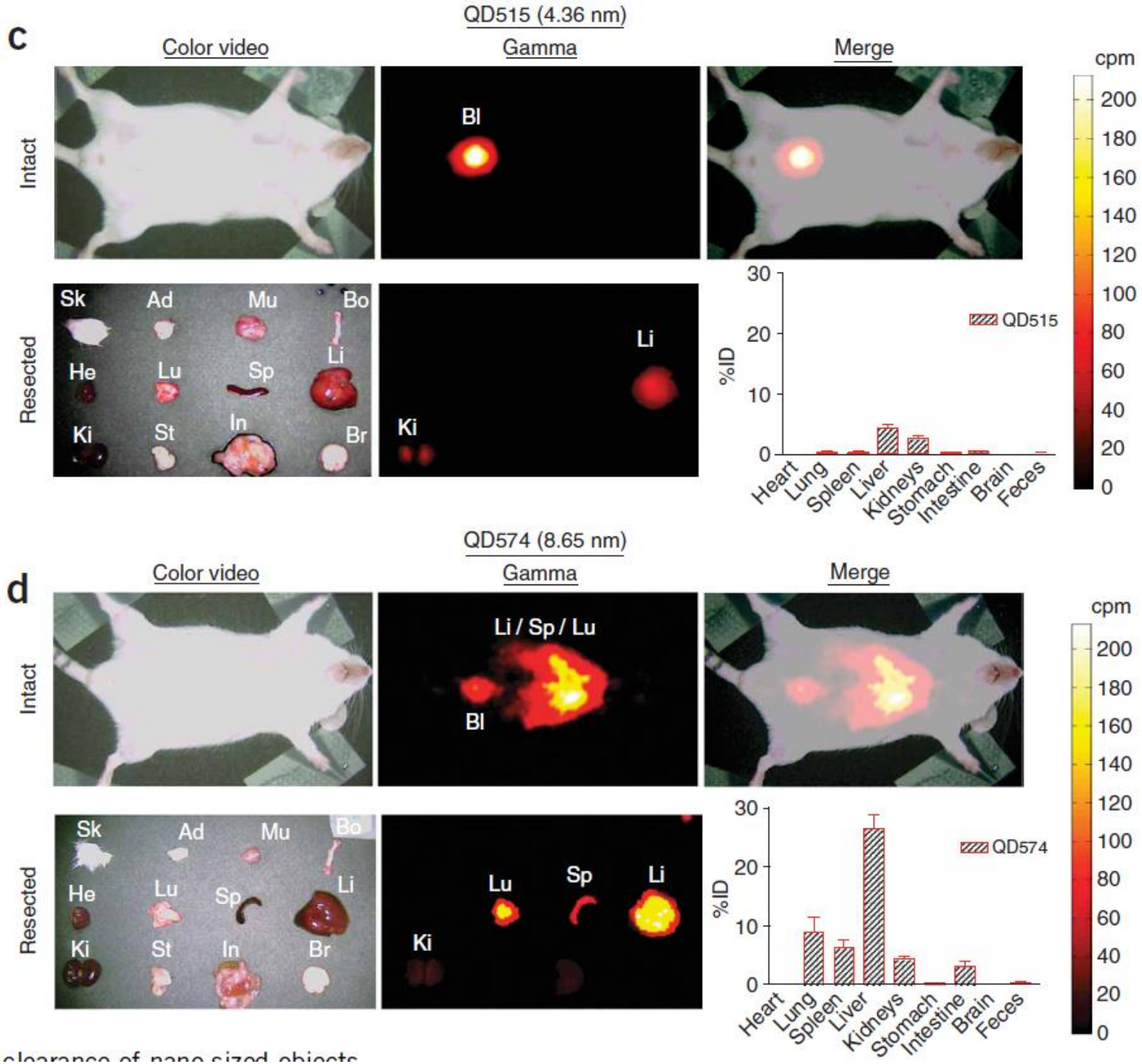

clearance of nano-sized objects

Hydrodynamic diameter vs. Blood half-life and Urine excreation

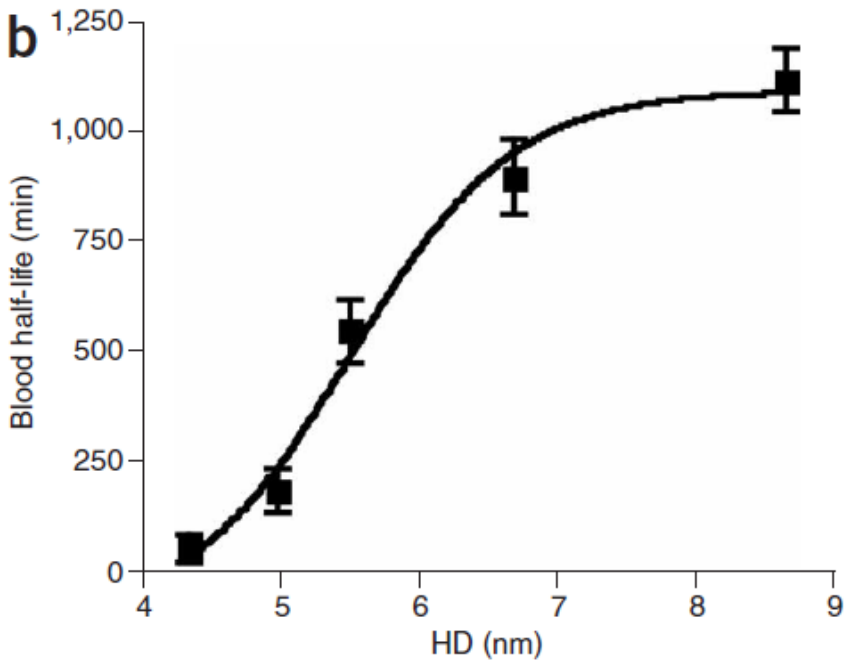

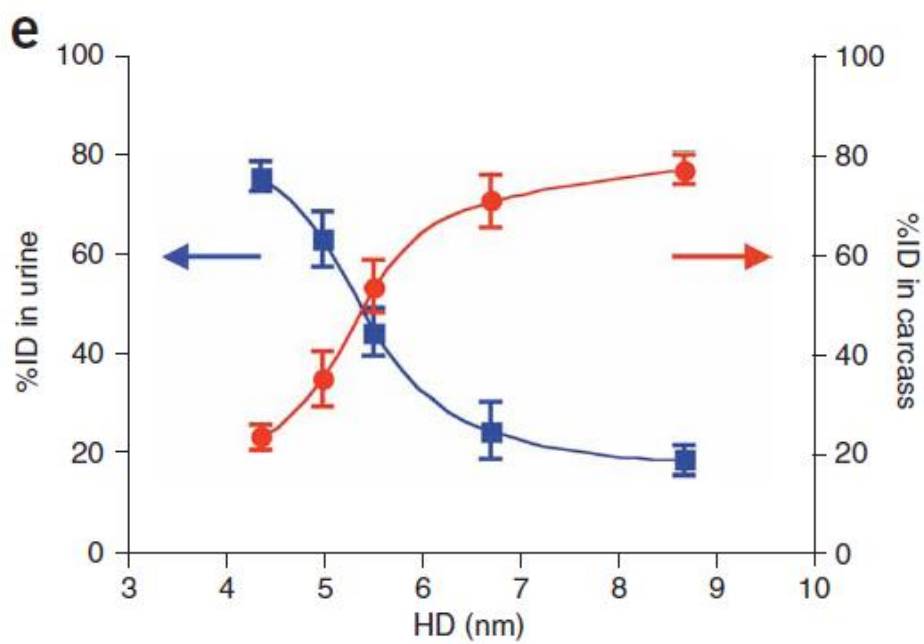

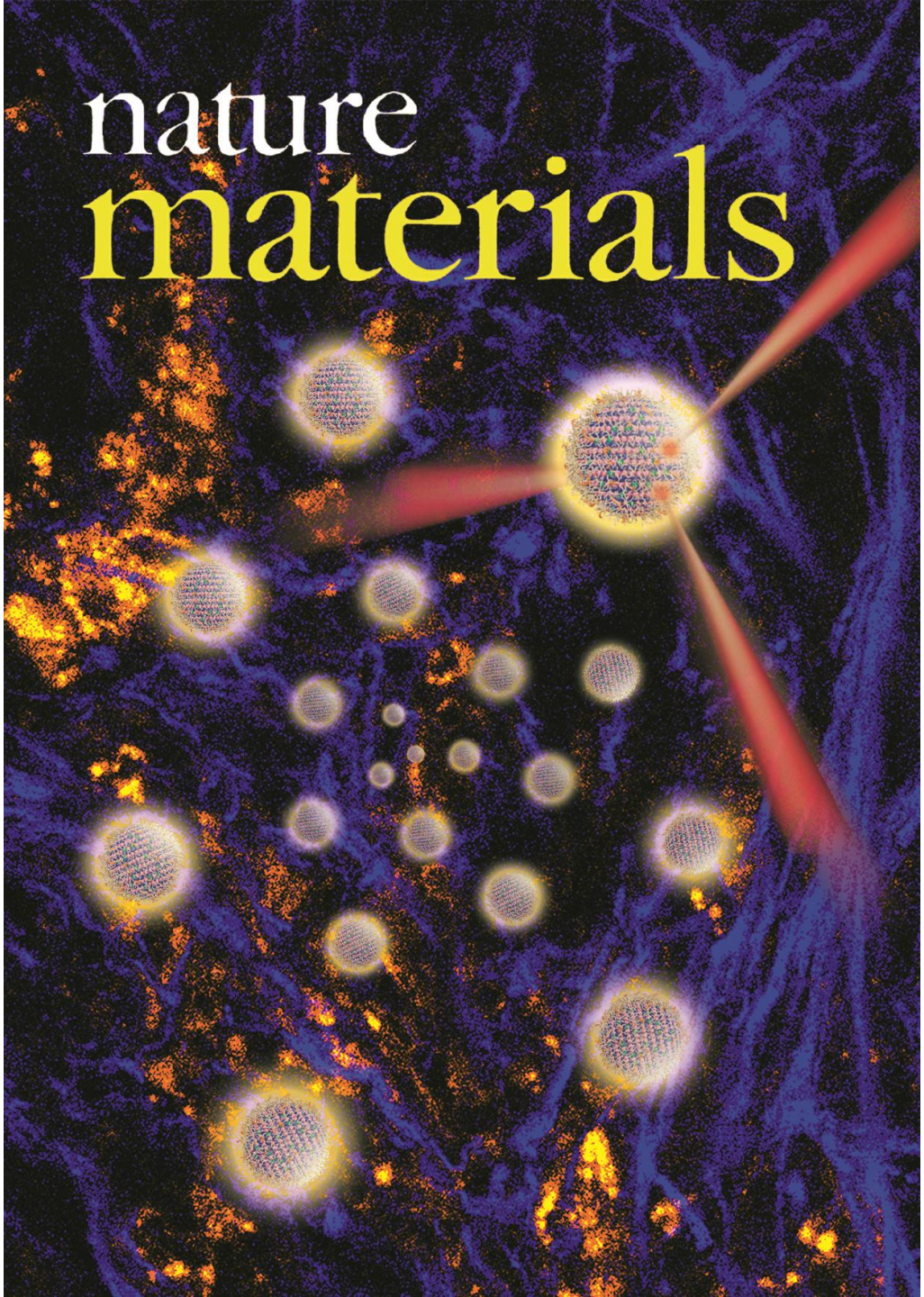

High-Resolution Three-Photon Biomedical Imaging using Bright Doped ZnS Nanocrystals

J. Yu et al.,
Nature Mater. **2013**, 12, 359.

NIR emitting window is appealing for biological optical imaging because of the low tissue absorption and scattering effects. typically at 650–900 nm

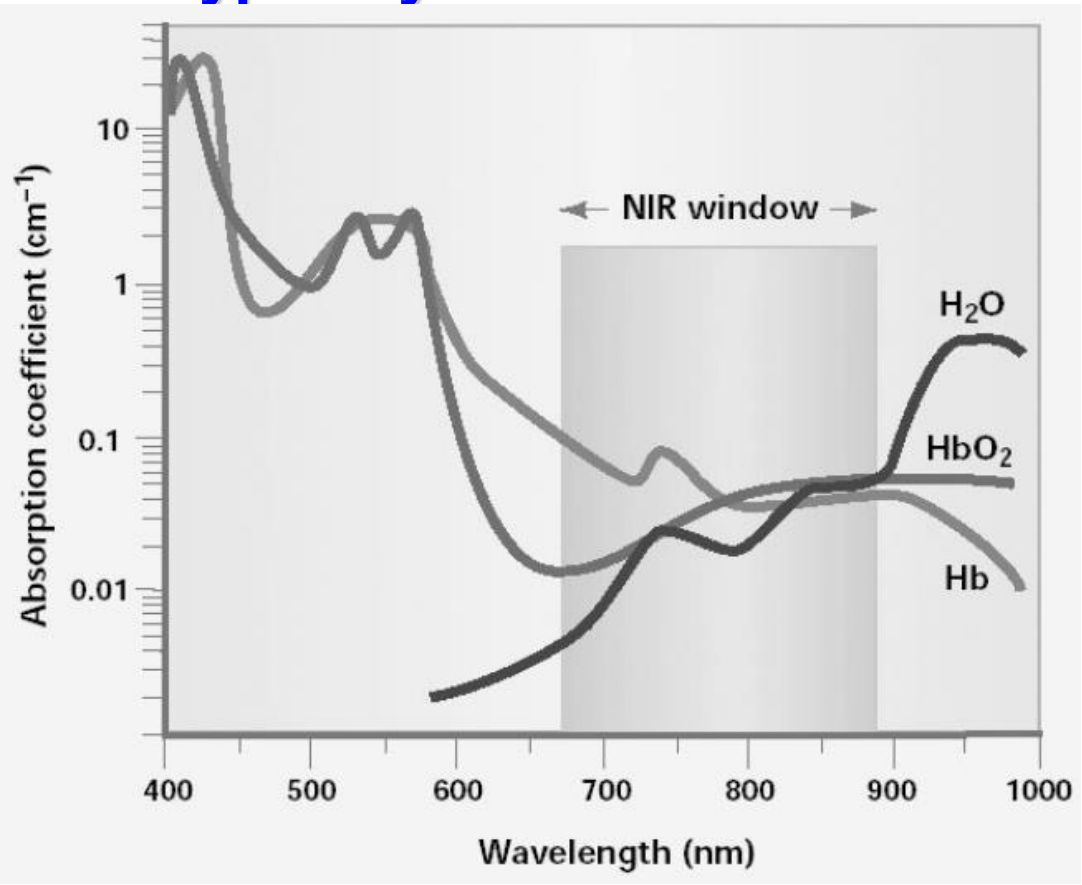

R. Weissleder, *Nature Biotechnol.* **2001**, *19*, 316.

NIR-imaging guided Surgery using NIR QDs (CdTe/CdSe QDs

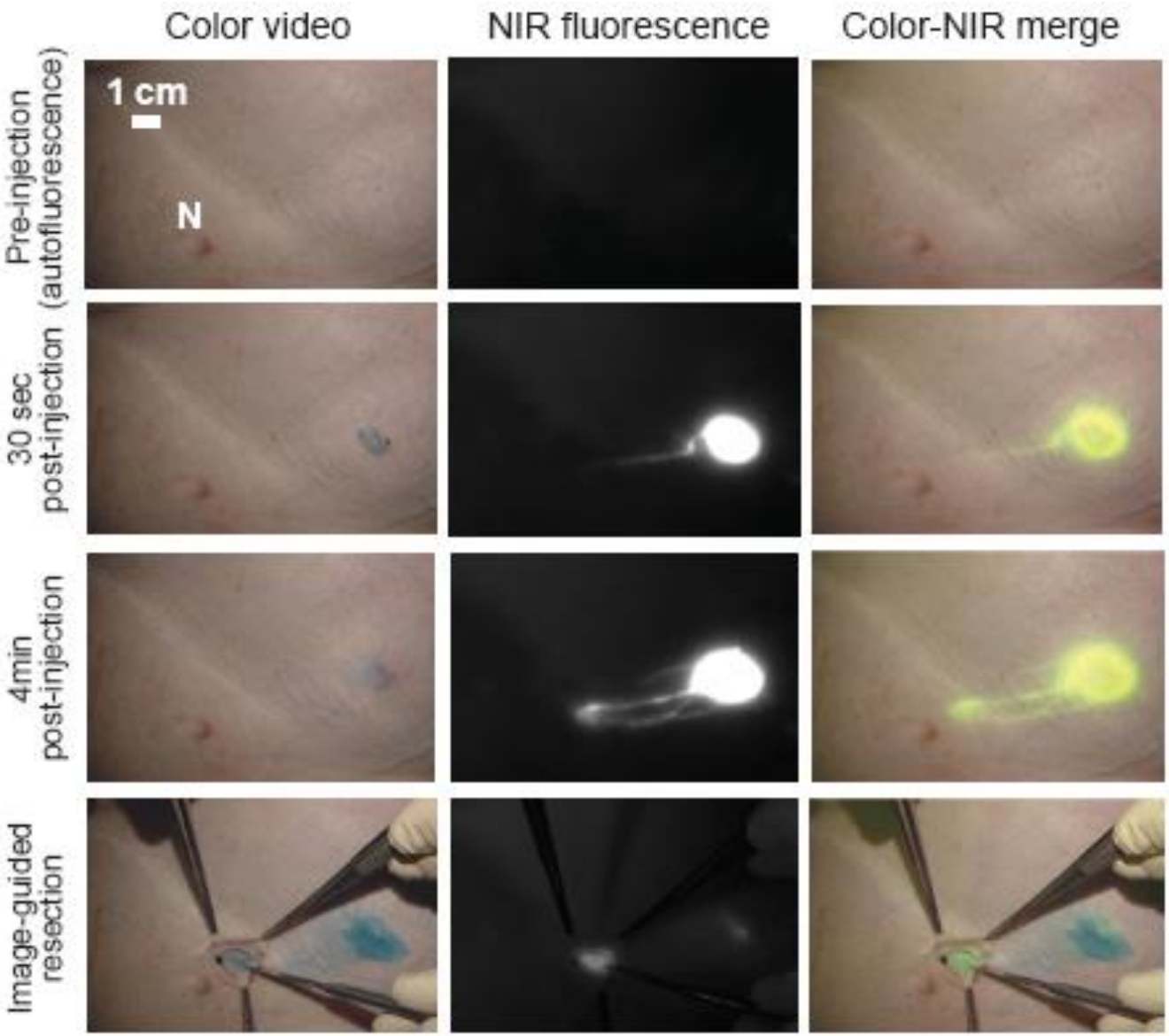

Sungjee Kim, Yong Taik Lim, ……., M. G. Bawendi, J. H. Frangioni, *Nature Biotechnology* **2004**, 22, 93.

Toxicity Issue of Semiconductor Nanocrystals

The in vivo accessible quantum dots are composed of toxic elements, and hardly degradable. Making smaller Q.D. < 6 nm requires more toxic element (Arsenic).

– Prof. Frangioni@MGH*Nat. Biotech*. Commentary 2011)

- Almost every fluorescence imaging semiconductor nanocrystal is composed of toxic elements (Cd, As, Se, etc.)

- **ZnS is a main-cover material to temporarily solve this problem.**

CdSe/ZnS, CdTe/ZnS
InP/ZnS, InAs/ZnS

3-photon imaging using non-toxic & bright Mn^{2+}-doped ZnS nanocrystals enables deeper tissue penetration *in vivo*.

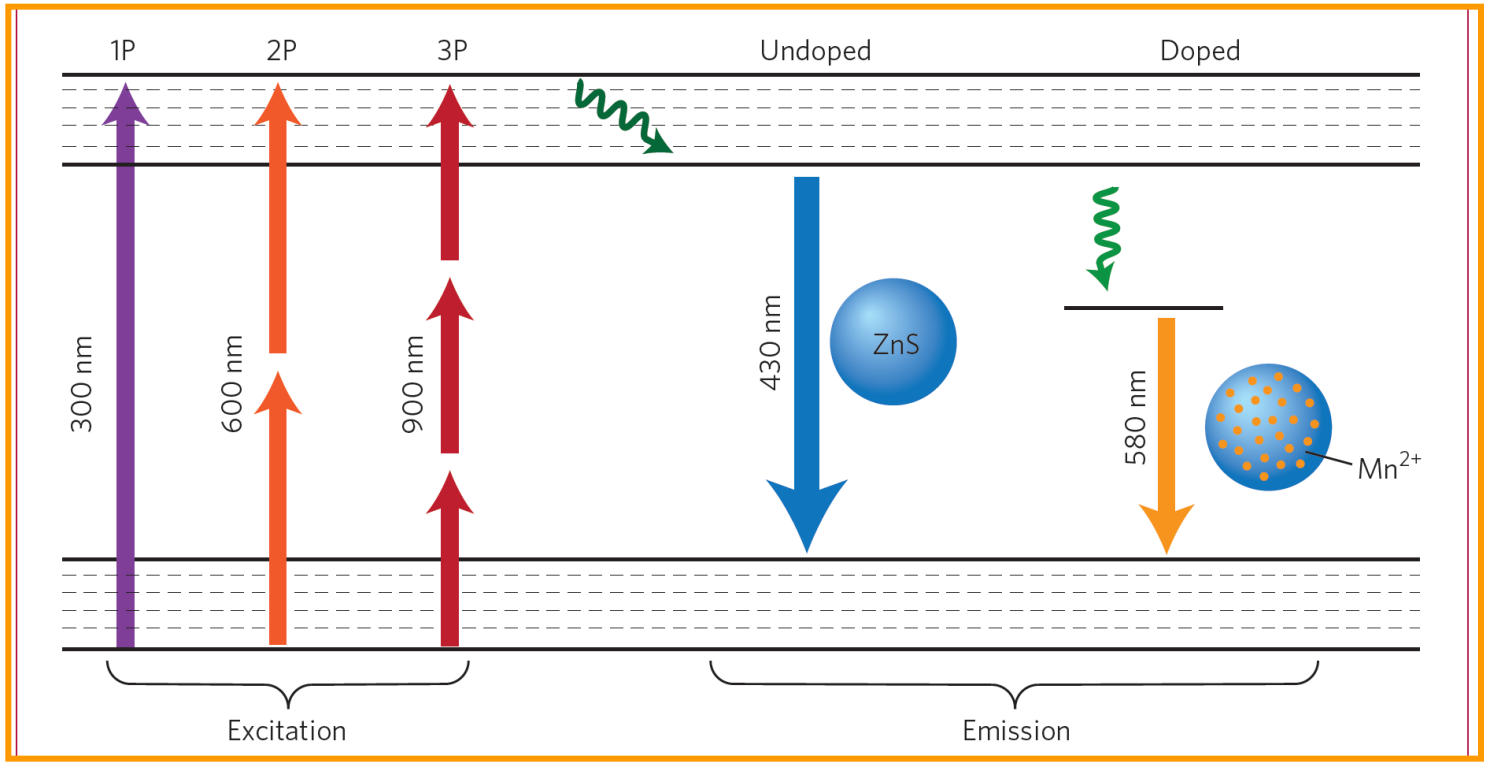

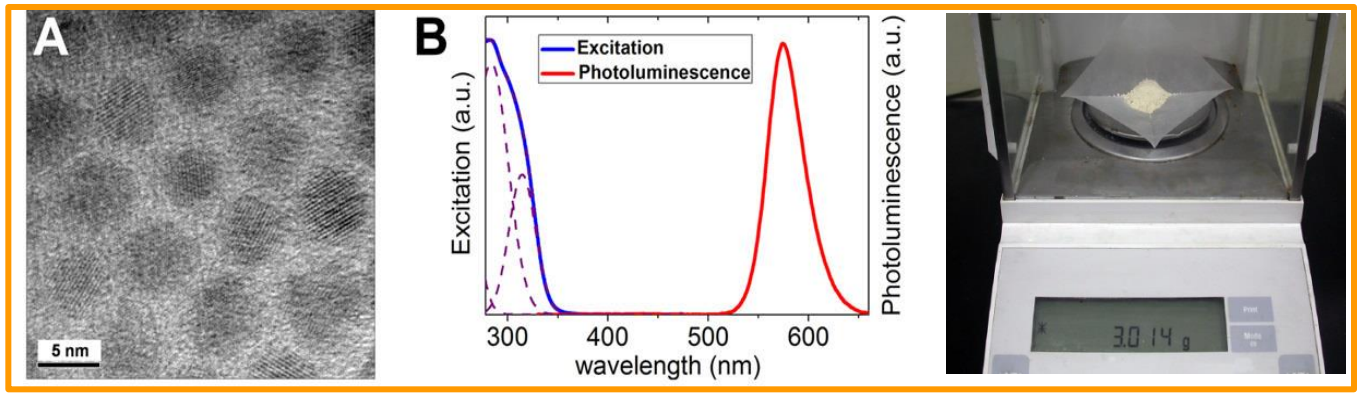

"News & Views in *Nature Mater.*," K. Zagorovsky, W. C. W. Chan, *Nature Mater.* **2013**, 12, 285.

3-photon fluorescence microscopy improves tissue penetration depth and resolution *in vivo*.

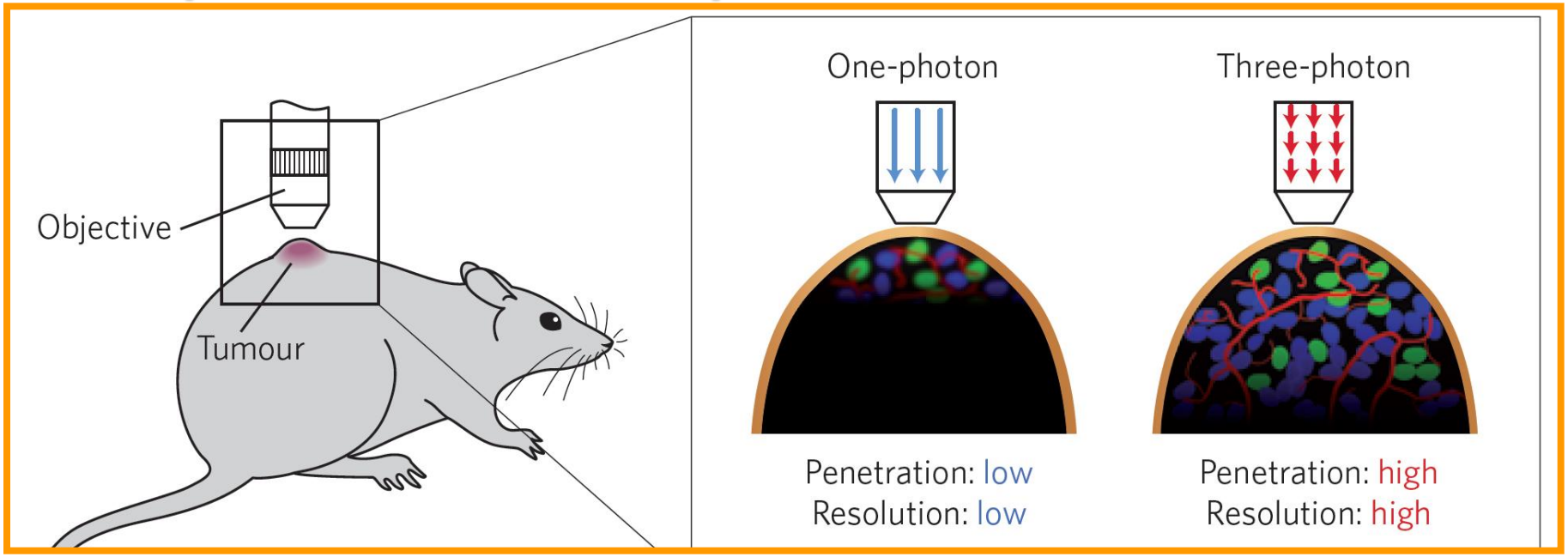

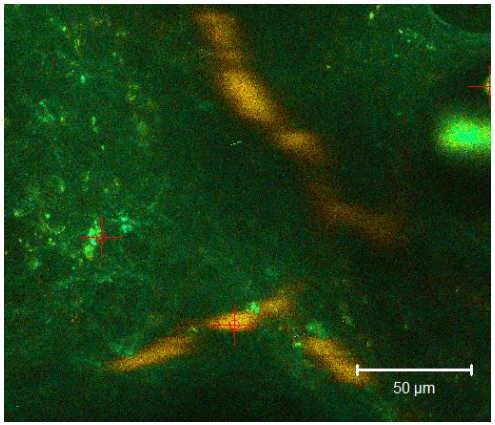

"News & Views in *Nature Mater.*," K. Zagorovsky, W. C. W. Chan, *Nature Mater.* **2013**, 12, 285.

Fluorescence Correlation Spectroscopy

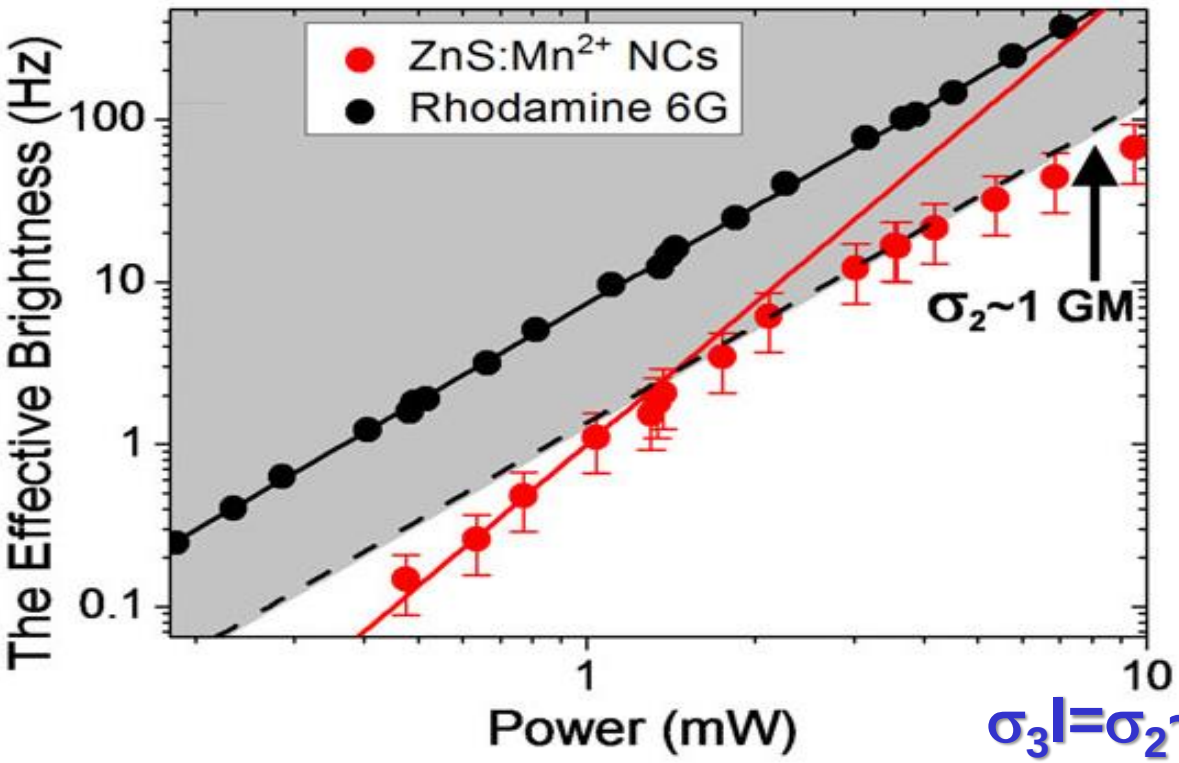

$\sigma_3 I = \sigma_2 \sim 1GM$ @ 1.3 mW

- The quantum mechanical probability of three-photon process is lower than that of one-photon and two-photon process.
  (3PA~The 5th order nonlinear optical process!)
- Due to large 3PA cross section of ZnS:Mn NCs, the 3PL brightness reaches to the two-photon brightness of 1 GM at low power of 1.3 mW.

3PL High-Resolution Imaging of ZnS:Mn NCs

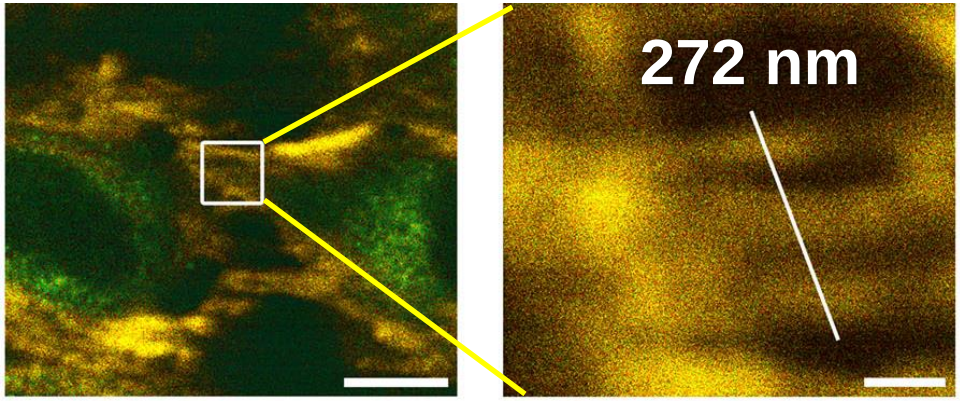

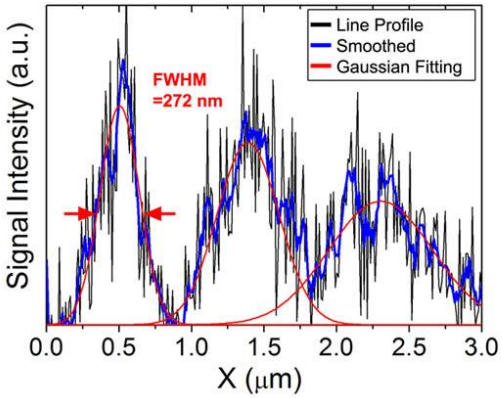

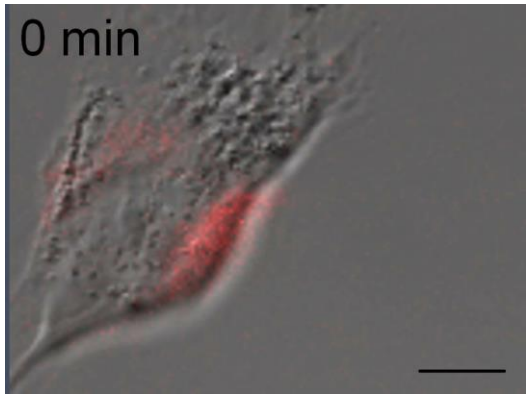

High-Resolution Imaging at non-saturation regime ⟷ **Temporal Imaging @ low power (1mW)**

3PL of ZnS:Mn NCs enables **high-resolution imaging** approaching theoretical limit of 3PL Imaging (**272 nm** for 950 nm NIR excitation).

The ability of live cellular imaging for 10 hours demonstrates **no phototoxicity** at the imaging condition owing to **low power excitation of 0.5 mW**.

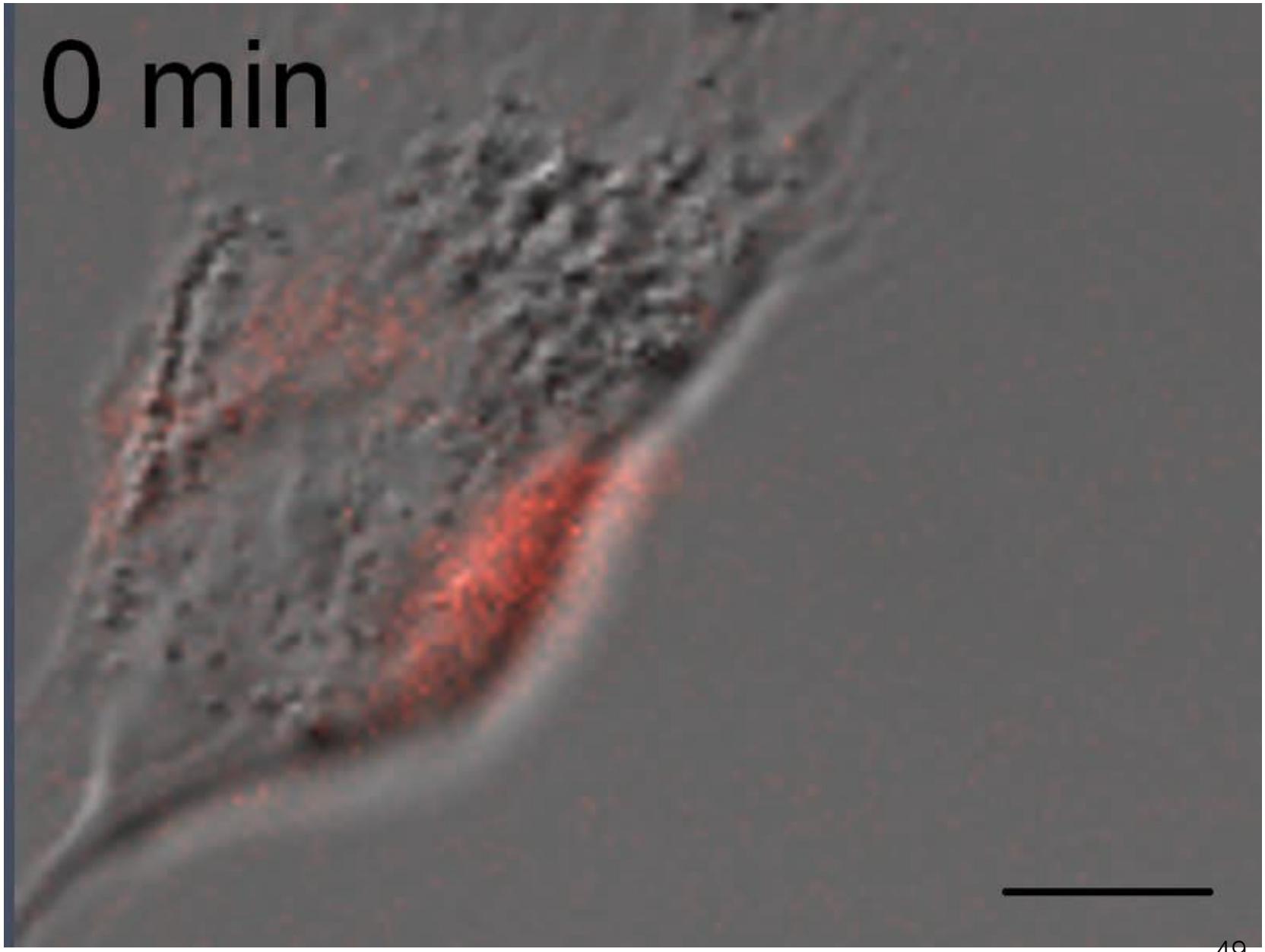
0 min

In Vivo 3PL Imaging of ZnS:Mn NC-RGD Conjugates

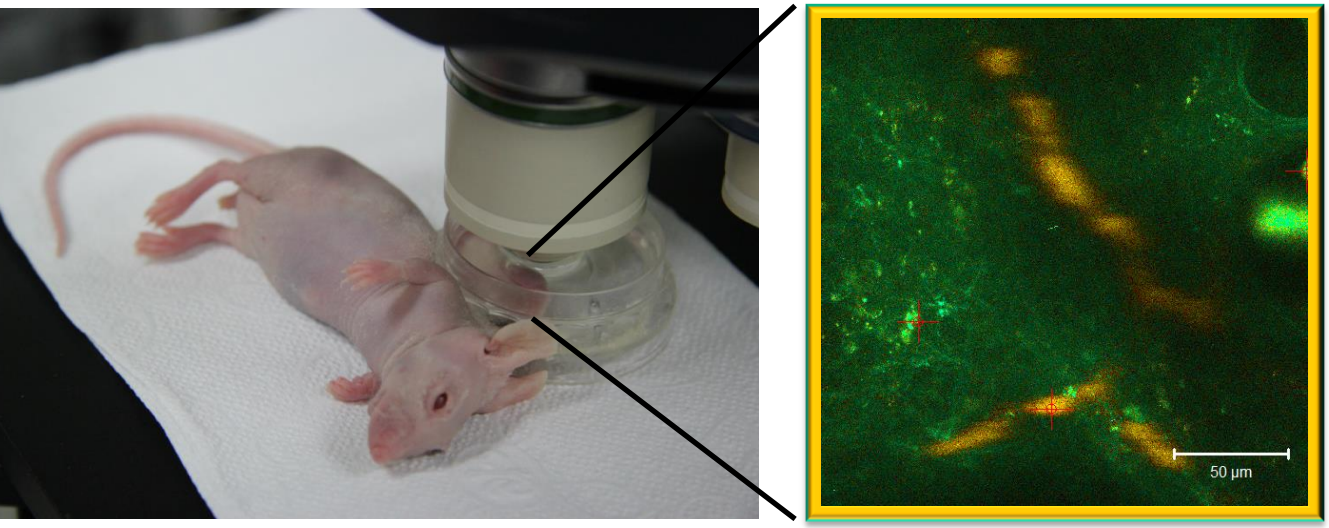

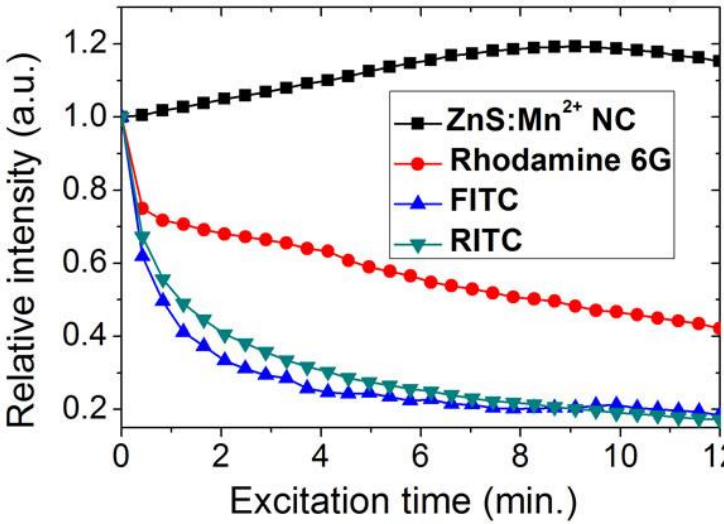

- High photostability of ZnS:Mn NCs enables in vivo 3PL imaging at high power (~10 mW).
- 3PL of RGD-conjugated ZnS:Mn NCs were visualized at the tumor vasculature due to the angiogenesis targeting.

Depth-projection of Tumor Vasculature

Background autofluorescence

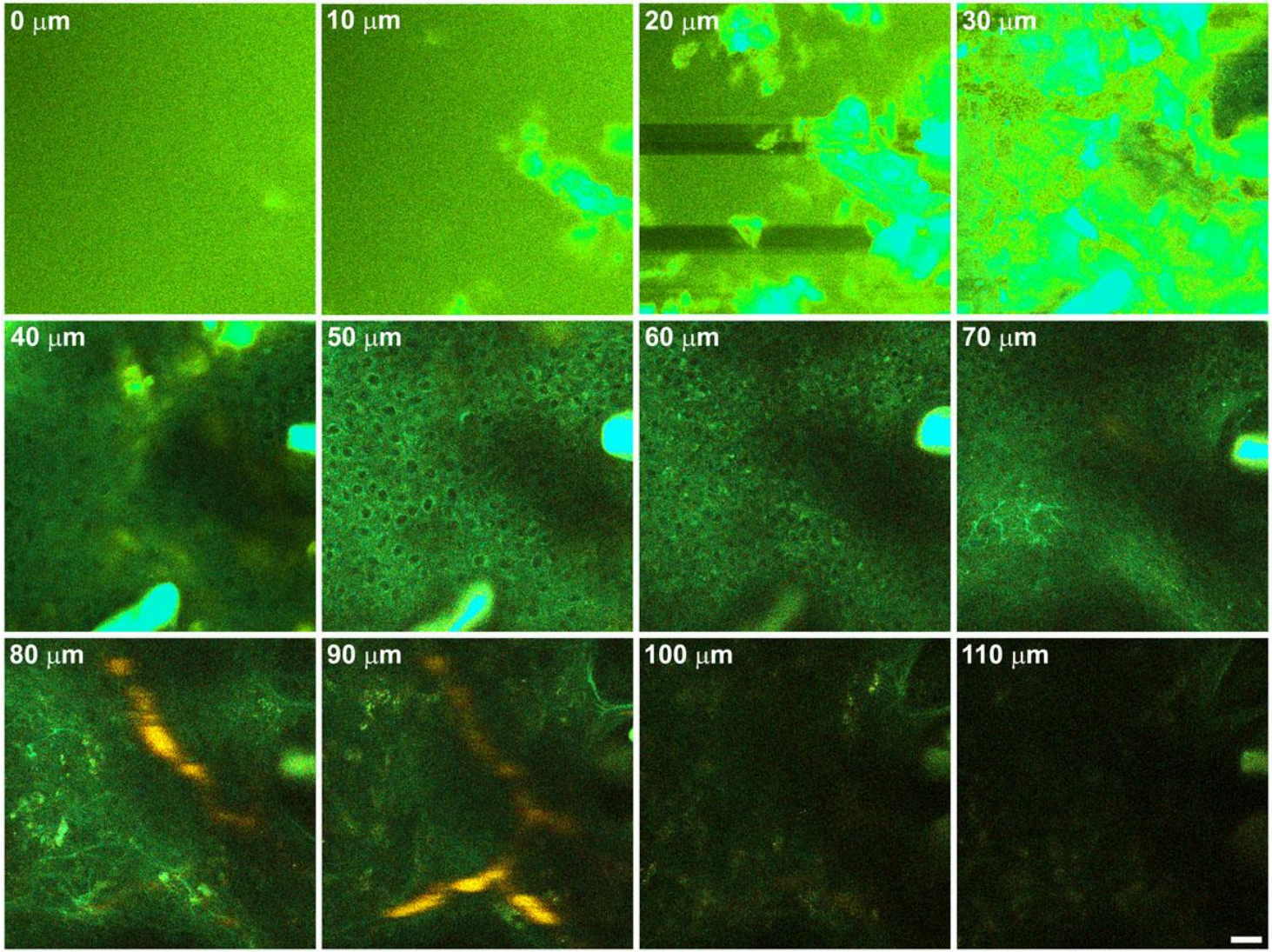

3PL of RGD-conjugated ZnS:Mn NCs can be imaged down to 100 μm even at the base of dermis (**Highly Scattering & Very Challenging**).

In Vivo 3PL Imaging of ZnS:Mn NC-targeting Tumor

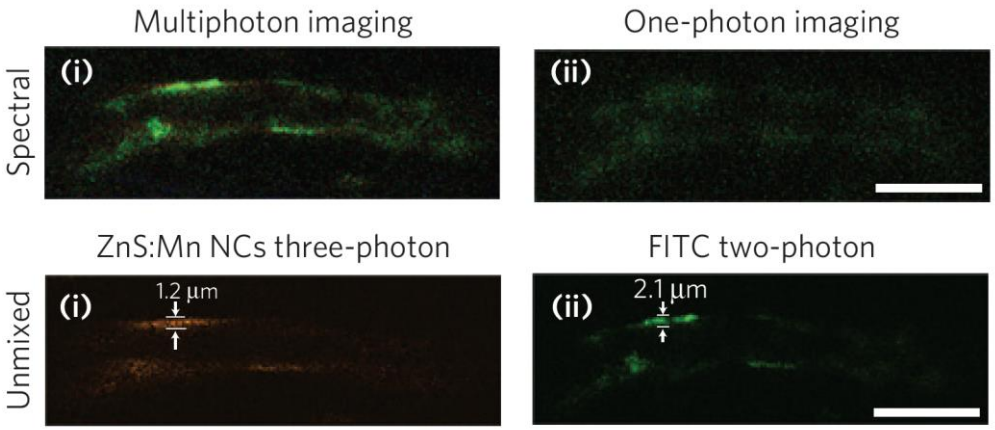

SHG from collagen fiber

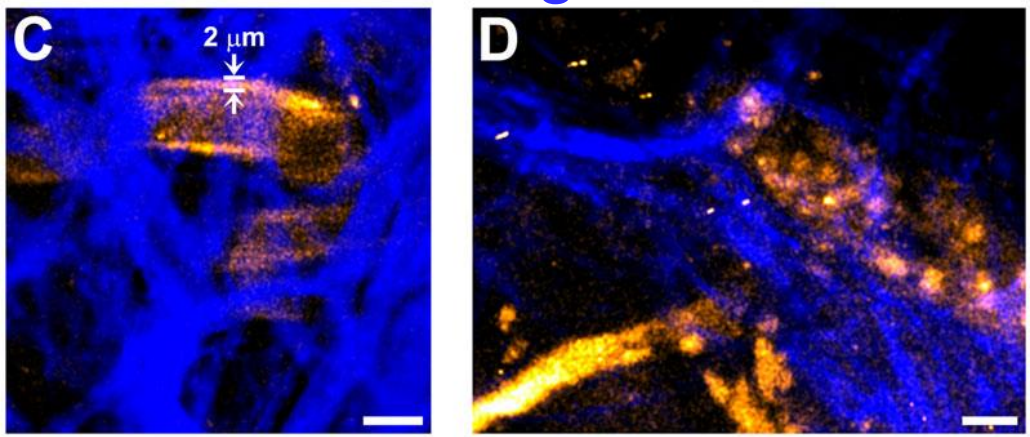

Endothelial Lining (µm resolution)

Extravasation (subcellular resolution)

- 3PL of ZnS:Mn NCs in tumor vasculature is **highly bright** & **spectrally distinguishable** from background fluorescence.

- 3PL Imaging of ZnS:Mn NCs-targeting Tumor at **µm & Subcellular Resolution.**

In Vivo Toxicity Examination of ZnS:Mn NCs

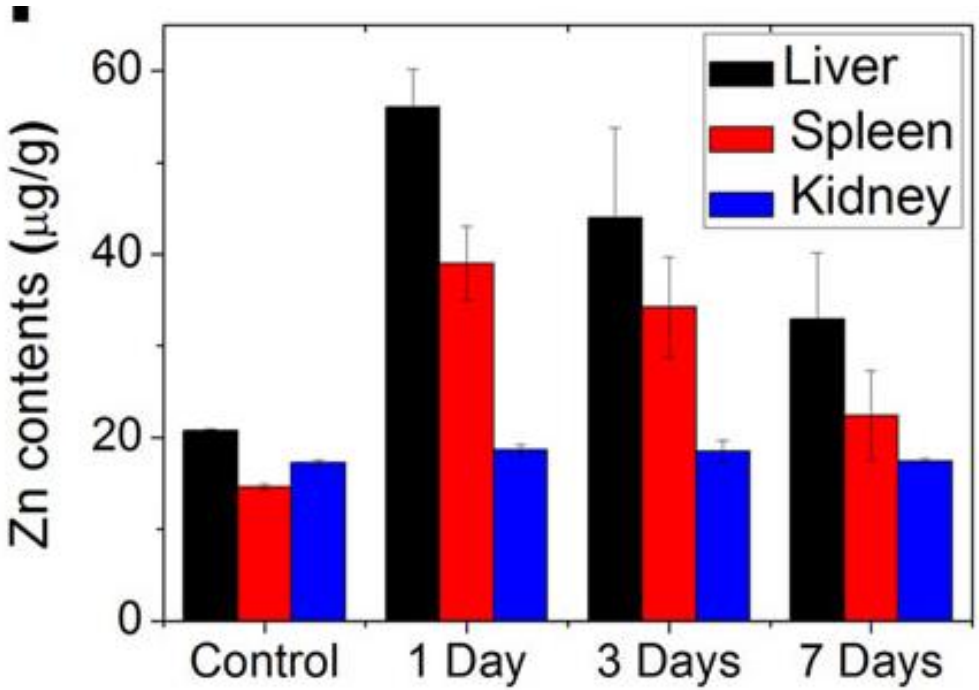

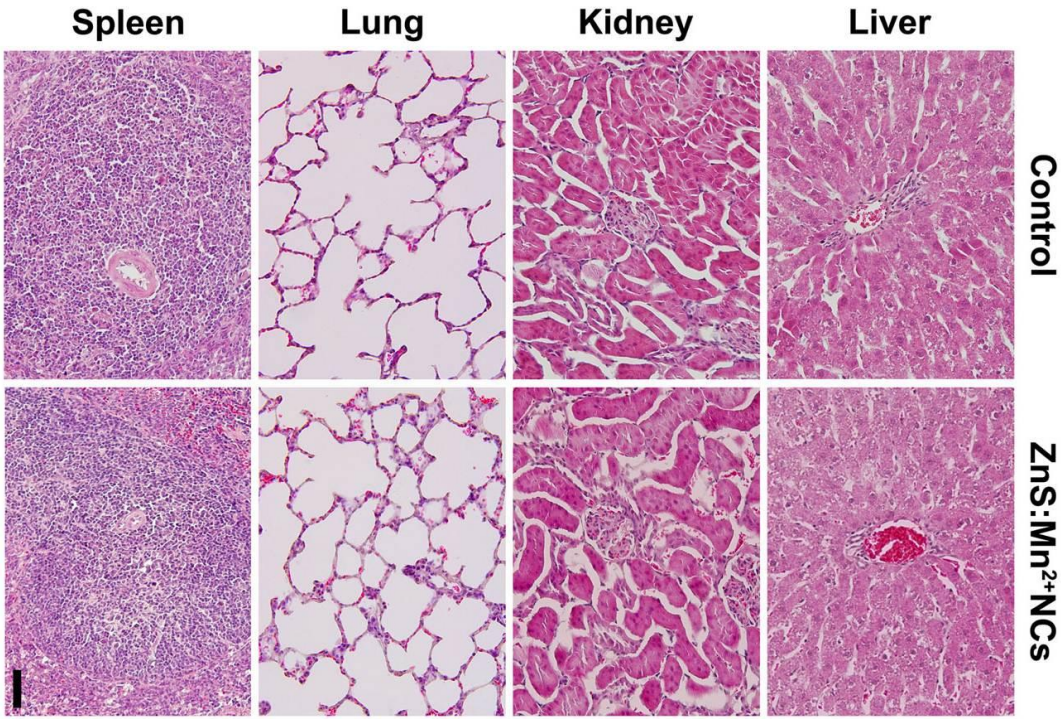

- The reticuloendothelial organs already contain non-negligible amounts of zinc ions (Biocompatibility of ZnS nanocrystals).
- The total amount of zinc ions is gradually decreased (Clearance of ZnS nanocrystals).
- The histological examination confirms no sign of in vivo toxicity (Biocompatibility of ZnS nanocrystals).